Preprint of chapter in the book "Out of Equilibrium Soft Matter: Active Fluids" https://doi.org/10.1039/9781839169465
《出平衡软物质：活性流体》一书的章节预印本 https://doi.org/10.1039/9781839169465

CHAPTER 9
第9章 活性流体的流变学
Rheology of active fluids

ALFREDO LANZARO,[a] LUIGI GENTILE,[b,*]
阿尔弗雷多·兰扎罗，[a] 路易吉·真蒂莱，[b,*]

[a] Institute for Advanced Rheology, Guangzhou University, 510006 Guangzhou, China. [b] Department of Chemistry, University of Bari "Aldo Moro", 70126 Bari, Italy
[a] 广州大学系统流变学研究所，中国广州 510006；[b] 化学系，巴里艾尔多·莫罗大学，意大利巴里 70126

*corresponding email: luigi.gentile@uniba.it
*通讯作者电子邮箱：luigi.gentile@uniba.it

Abstract. This chapter on the rheology of active fluids is an attempt to correlate theoretical and experimental work. A considerable amount of the oretical work and most of the experimental data focus on the rheology of active fluids in a Newtonian matrix, which displays uncommen macroscopic rheological behaviors, such as the apparent superfluid-like state of the pusher suspensions. The failure of the "scallop theorem" for reciprocal swimmers in a non-Newtonian matrix is highlighted. Finally, recent findings concerning the turbulent-like behaviour in concentrated systems are described in detail.

摘要： 本章探讨活性流体的流变学，旨在将理论研究与实验工作联系起来。大量理论研究和大多数实验数据都集中于牛顿基质中的活性流体流变学，这类流体呈现出不同寻常的宏观流变行为，例如推型游动体悬浮液表现出的表观超流体状态。本文着重讨论非牛顿基质中往复游动体的"扇贝定理"失效问题。最后，详细介绍浓缩体系中类湍流行为的最新发现。

Book Series: Soft Matter Science
丛书：软物质科学
Out of Equilibrium Soft Matter: Active Fluids
非平衡软物质：活性流体
Edited by Luigi Gentile, Christina Kurzthaler and Howard A. Stone
主编Luigi Gentile, Christina Kurzthaler 和 Howard A. Stone
Out of Equilibrium Soft Matter: Active Fluids
出平衡软物质：活性流体
Edited by Luigi Gentile, Christina Kurzthaler and Howard A. Stone
主编Luigi Gentile, Christina Kurzthaler 和 Howard A. Stone
© Royal Society of Chemistry 2020
© 英国皇家化学会 ID 英国皇家化学会 2020
Published by the Royal Society of Chemistry, www.rsc.org
2020年出版，出版方为英国皇家化学会

Contents 目录

1.1 Introduction 2
1.1.1 Low Reynolds number swimming and viscous dominated flows
1.1.2 Stokeslet, Stresslet and Rotlet
1.1.3 Turbulence
1.2 Rheometry of active fluids and the problem of sensitivity 5
1.3 The apparent viscosity of active particle suspensions 7
1.3.1 Concentration dependence of the apparent viscosity 11
1.4 Concentrated Systems and the Onset of Turbulence 11
1.5 Rheology of active polar liquid crystals 14
1.6 Matrix viscoelasticity affects the swimming behaviour 16
1.7 Perspectives 21

1.1 Introduction 1.1 引言

The most significant parameter in rheology of complex fluids is the Deborah number, $\mathscr{D}$. It is defined as the ratio between the characteristic (relaxation) time of the fluid, λ, and the observation time, t_o: $\mathscr{D} = \lambda/t_o$. Here, t_o represents the characteristic time scale of the material to the applied stress (or deformation). Depending on t_o, a flow can therefore be "slow" or "fast" if $\mathscr{D} \ll 1$ or $\mathscr{D} \gg 1$ respectively.

Fluids can generally be divided in: (i) Newtonian fluids, where the relation between the shear stress, σ, and the shear rate, $\dot{\gamma}$, is linear, (ii) Pseudoplastic (shear thinning) fluids, usually described by the Oswald and de Waele power law equation $\sigma = K(T)\dot{\gamma}^a$, where a, the flow behavior index, is < 1, and the yield stress $\sigma_y = 0$, while $K(T)$ is the consistency index at a fixed temperature T, (iii) Dilatant (shear thickening) fluids where the value a of the Oswald and de Waele power law is > 1 and $\sigma_y = 0$, (iv) Yield-pseudoplastic and Bingham plastic fluids, which are shear thinning and shear thickening, respectively but both showing a non-vanishing yield stress, i.e., $\sigma_y \neq 0$. In the case of Newtonian fluids, the flow dynamics can be fully described by the Navier-Stokes equations, for which unfortunately an exact solution is not always available due to the complexity of the flow turbulence (high Reynolds number, Re), even if various perturbation schemes have been adopted.[3,4]

The relation between the apparent viscosity, η_{app}, and the volume fraction, ϕ, of passive particles is typically described by the Einstein,[5] Batchelor,[6] and Krieger-Dougherty[7] equations. On the other hand, a rich rheological phenomenology is observed for lyotropic liquid crystals and polymers when an external force or flow field is imposed. For example, the disturbance arising from the applied flow field can induce a lamellar-to-vesicle transition under shear.[8] Such flow-induced structural changes lead in some cases to regular oscillations of the measured viscosity.[9] This suggests that a further class of materials, characterized by a well-defined time dependence of the measured shear viscosity, should also be considered.

Active fluids can act as shear thinning, shear thickening, shear-unstable fluids or superfluids, depending on the relevant dimensionless parameters.[10] Here, we focus on the simplest case of a suspension of active particles in a Newtonian fluid and we show how the diffusive transport of the active particles and the disturbance flows induced by the individual

particles. The latter factor is intrinsically related to the concentration and shape of the active particles. Finally, the medium in which the particles are "swimming" is also of primary importance. In most of the literature the medium is assumed to be a viscous Newtonian fluid. The rheology of active fluids is usually referring to bacteria and algae organisms as main examples along with synthetic designed particles.

最后一个因素与活性粒子的浓度和形状密切相关。此外，粒子“游动”其中的介质也至关重要。在大多数文献中，介质都被假定为黏性牛顿流体。活性流体流变学通常以细菌和藻类生物为主要例子，同时也包括人工设计粒子。

1.1.1 Low Reynolds number swimming in a Newtonian medium

1.1.1 牛顿介质中的低雷诺数游动

The motion of fluids surrounding swimming bacteria is modeled by means of the Cauchy equations expressing the conservation of momentum and mass,[11]

游动细菌周围流体的运动通过表达动量守恒和质量守恒的柯西方程组进行建模，[11]

$$\rho\left(\frac{\partial \mathbf{u}}{\partial t}+\mathbf{u}\cdot\nabla\mathbf{u}\right)=-\nabla\cdot\sigma-\nabla p+\rho\mathbf{g} \tag{1.1a}$$

$$\nabla\cdot\mathbf{u}=0 \tag{1.1b}$$

where t is time, ρ is the fluid density, $\mathbf{u}$, p, and σ are the velocity, pressure, and stress tensor fields respectively, and $\mathbf{g}$ is the body acceleration field due to the presence of external forces (usually gravity). The left hand term of Eq. (1.1a) is often written in terms of the material derivative of the velocity,

其中 t 是时间，ρ 是流体密度，$\mathbf{u}$、p 和 σ 分别是速度、压力和应力张量场，而 $\mathbf{g}$ 是由外力（通常为重力）产生的体加速度场。方程(1.1a)左侧的项通常用速度的物质导数表示，

$$\frac{D\mathbf{u}}{Dt}\simeq\frac{\partial \mathbf{u}}{\partial t}+\mathbf{u}\cdot\nabla\mathbf{u}, \tag{1.2}$$

which expresses the rate of change of $\mathbf{u}$ as computed from a velocity frame co-moving with the fluid. In order to close the problem a constitutive equation must be specified relating σ with the strain rate tensor $\mathbf{E}=\frac{1}{2}\left(\nabla\mathbf{u}+\nabla\mathbf{u}^{T}\right)$. In case of Newtonian fluids, the stress is linear in $\mathbf{E}$, that is,

它表示 $\mathbf{u}$ 相对于与流体共同运动的速度参考系所计算出的变化率。为了使问题闭合，必须指定一个本构方程，将 σ 与应变率张量 $\mathbf{E}=\frac{1}{2}\left(\nabla\mathbf{u}+\nabla\mathbf{u}^{T}\right)$ 联系起来。对于牛顿流体，应力与 $\mathbf{E}$ 呈线性关系，即，

$$\sigma=-2\eta\mathbf{E}, \tag{1.3}$$

where η is the viscosity of the fluid. By substituting Eq. (1.3) into Eq. (1.1a), we obtain the Navier-Stokes equations,

其中 η 是流体的黏度。将方程(1.3)代入方程(1.1a)可得到纳维-斯托克斯方程组，

$$\rho\left(\frac{D\mathbf{u}}{Dt}\right)=\eta\nabla^{2}\mathbf{u}-\nabla p+\rho\mathbf{g} \tag{1.4a}$$

$$\nabla\cdot\mathbf{u}=0. \tag{1.4b}$$

Eq. (1.4a) can be made dimensionless as

方程(1.4a)可写成无量纲形式，

$$\frac{D\mathbf{u}^{*}}{Dt^{*}}\equiv\frac{1}{Re}\nabla^{*2}\mathbf{u}^{*}-\nabla^{*}p^{*}+\frac{1}{Fr^{2}}\mathbf{g}^{*} \tag{1.5}$$

where the asterisk indicates a non-dimensional quantity, and $Re=\rho UL/\eta$, and $Fr=U/\sqrt{gL}$, with L a characteristic lengthscale, u is the particle velocity, R is the particle

其中，星号表示无量纲量，而 $Re=\rho UL/\eta$ 以及 $Fr=U/\sqrt{gL}$，其中 L 为特征长度尺度，u 为粒子速度，R 为粒子

radius, and η is the fluid viscosity that for a suspension of particles is the Newtonian viscosity. The Reynolds Re and Froude Fr numbers express the ratio between inertial and viscous forces and the ratio between fluid inertia and the strength of the body force, respectively. In the density-matching approach $Fr \to \infty$ in the case of swimming bacteria with $u \approx 10\ \mu$m/s, $L \approx 10\ \mu$m and density close to that of the fluid. Moreover, as the kinematic viscosity of water is $\nu = \eta/\rho \approx 10^{-6}$ m^2/s, we also obtain $Re \ll 1$. Therefore, Eq. (1.5) simplifies to the Stokes equation,

雷诺数 Re 和弗劳德数 Fr 分别表示惯性力与黏性力之比，以及流体惯性与体积力强度之比。在密度匹配方法中，对于速度为 $u \approx 10\ \mu$m/s、特征长度为 $L \approx 10\ \mu$m 且密度接近流体密度的游动细菌，$Fr \to \infty$。此外，由于水的运动黏度为 $\nu = \eta/\rho \approx 10^{-6}$ m^2/s，因此 $Re \ll 1$。因此，式 (1.5) 简化为斯托克斯方程，

$$\mathbf{0} = \nabla^{*2}\mathbf{u}^* - \nabla p^*. \tag{1.6}$$

Eq. (1.6) suggests that the body experiences no net force or torque throughout its motion. Moreover, Stokes equations are linear and independent of time. As a consequence, if the body undergoes a reciprocal motion that does not break the time-reversal symmetry, like the opening and closing of a scallop, it will not experience any net displacement[12–14]. To achieve self-propulsion, swimmers rather need to perform non-reciprocal types of propulsion. Examples include, but are not limited to, wave-like deformations of the body[14] or of the cilia[15,16]. Moreover, the "scallop theorem" is only valid for a single swimmer undergoing inertialess motion through a Newtonian medium. In particular, a violation of the latter condition allows for net displacement also in the case of symmetric swimmers, as will be seen in Section 1.6. For a detailed hydrodynamic description of swimming cells see Chapter **??**.

式 (1.6) 表明，物体在整个运动过程中所受的合力和扭矩均为零。此外，斯托克斯方程是线性的，且与时间无关。因此，如果物体进行不破坏时间反演对称性的往复运动，例如扇贝的张开和闭合，它就不会产生任何净位移[12–14]。游动体若要实现自推进，则需要采用非往复推进方式。例如，但不限于，身体的波状形变[14]或纤毛的波状形变[15,16]。此外，"扇贝定理"仅适用于在牛顿介质中进行无惯性运动的单个游动体，特别是，若不满足后一条件，即使是对称游动体也能产生净位移，这一点将在第 1.6 节中看到。有关游动细胞的详细流体动力学描述，请参阅第 ?? 章。

1.1.2 Stokeslet, Stresslet and Rotlet

1.1.2 斯托克斯单极子、应力偶极子与旋转单极子

Stokes equations are linear, implying that any flow can be represented through a combination of simpler flows. The latter is usually chosen as a uniform flow, a point force (Stokeslet), and their derivatives[17]. The derivative of the Stokeslet is the flow from a force dipole. Usually, the force dipole is decomposed into a symmetric component called the **stresslet** and an antisymmetric component called the **rotlet**. The former represents pure strain flow, while the latter is the flow from a point torque. The Stokeslet, stresslet, and rotlet are singularities in the Stokes flow. The full regularization of the singularities for active particles is provided by Ghose and Adhikari[18] and Saintillan[19] for the rotation of the flagellar bundle of the *Escherichia coli* bacterium and thrust $-F_0\mathbf{p}$ with particle orientation $\mathbf{p}$, where l is a microscopic length scale of the force $F_0\mathbf{p}$ exerted by the cell body as it translates through the fluid. This extensile force dipole results in a net stresslet with magnitude $\zeta \approx -F_0 l$, where l is a characteristic length on the order of the cell size. The negative sign of ζ indicates a **pusher**, which uses its flagellar tail to push itself through the fluid, while a positive sign would indicate a **puller**. ζ is often addressed as "activity coefficient" or swimming stresslet. The stresslet describes the single-cell disturbance very well in the far-field,[20] however, near the cell body a rotlet dipole arises due to the equal and opposite torques exerted by the flagellar bundle and cell body as they counter-rotate.[21]

斯托克斯方程是线性的，这意味着任意流动都可以表示为若干较简单流动解的组合，例如均匀流、点力流（斯托克斯单极子）及其导数。斯托克斯单极子的导数对应力偶极子产生的流动。通常，力偶极子可分解为称为应力偶极子的对称分量，以及称为旋转单极子的反对称分量[17]。前者表示纯应变流，后者则是点力矩产生的流动。斯托克斯单极子、应力偶极子和旋转单极子都是斯托克斯流中的奇点。Ghose 和 Adhikari[18] 以及 Saintillan[19] 完整阐述了活性粒子奇点的理论：大肠杆菌鞭毛束的旋转会产生净推力 $-F_0\mathbf{p}$，其方向沿颗粒取向 $\mathbf{p}$，当细胞体在流体中平移时；这一推力必须与其受到的黏性阻力 $F_0\mathbf{p}$ 相平衡。这种伸展型力偶极子会产生净推力 $-F_0\mathbf{p}$，其中 $\mathbf{p}$ 为细胞取向，l 是与细胞尺寸同量级的特征长度。s 为负值表示这是推型游动体，它利用鞭毛尾推动自身在流体中前进；若 s 为正值，则表示这是拉型游动体。s 通常称为"活性系数"或游动应力偶极子。应力偶极子能够很好地描述远场中的单细胞扰动[20]。然而，在细胞体附近，由于鞭毛束和细胞体反向旋转时施加了大小相等、方向相反的扭矩，因此会产生旋转偶极子[21]。

1.1.3 Turbulence

1.1.3 湍流

To describe active fluids, or more properly the flow of active particles in a Newtonian, and passive fluid, several approaches have been adopted. One approach is to describe the phenomenol-

为描述活性流体的流动，或者更准确地说，描述活性粒子在牛顿型被动流体中的流动，人们采用了多种方法。其中一种方法是用现象学方式描述活性体

ogy of the active states in terms of fourth- and higher-order expansions of the Navier-Stokes equations[22–24].

$$\nabla \cdot \mathbf{u} = 0 \tag{1.7a}$$

$$\rho\left(\frac{\partial \mathbf{u}}{\partial t} + \lambda_0 (\mathbf{u}\cdot\nabla)\mathbf{u}\right) = -\nabla p + \lambda_1 \nabla \mathbf{u}^2 - \left(A + C|\mathbf{u}|^2\right)\mathbf{u} + \eta_0 \nabla^2 \mathbf{u} - \eta_2 \nabla^4 \mathbf{u} + \rho \mathbf{g} \tag{1.7b}$$

式 1.7b 中的 $(A+C|\mathbf{u}|^2)\mathbf{u}$ 表示一个四次朗道速度势[25–27]，它考虑了通常由头尾不对称性导致的极性排列偏好。然而，游动细菌悬浮液中只在局部出现极性有序，而非全局出现这一事实[28–30]表明，还存在其他不稳定机制[31]，这些机制通过 A_1 项加以考虑。黏度系数 η_0 和 η_2 是对称无迹张量 $\mathbf{E}$ 张量（有时称为变形梯度）的项，其定义为[23]

The term $(A+C|\mathbf{u}|^2)\mathbf{u}$ in Eq. 1.7b represents a quartic Landau velocity potential[25–27] that accounts for the favored polar alignment usually due to the head-tail asymmetries. However, the fact that polar ordering appears only locally but not globally in suspensions of swimming bacteria[28–30] suggests that other instability mechanisms, that are considered through the λ terms. The viscosity coefficients η_0 and η_2 are terms of the symmetric and traceless rate-of-strain $\mathbf{E}$ tensor (sometimes called deformation gradient) defined as[23]

$$E_{ij} = \eta_0\left(\partial_i u_j + \partial_j u_i\right) - \eta_2 \nabla^2\left(\partial_i u_j + \partial_j u_i\right) + S\left(u_i u_j - \frac{\delta_{ij}}{d}|\mathbf{u}|^2\right). \tag{1.8}$$

式(1.8)右侧的最后一项是流动导致的活性应力的一个与 d 维无关的 d 维平均场近似，其中 δ_{ij} 是克罗内克张量。S 项不会影响模型的线性稳定性，但它考虑了活性粒子可作为推型游动体（$S<0$）发挥作用，例如 *E. coli*[32–34] 或枯草芽孢杆菌，也可作为拉型游动体（$S>0$）发挥作用，例如莱因衣藻。[32,35] 最后，式(1.7b)中的 A_0 和 A_1 等于 $A_0 = 1-S$ 和 $A_1 = -\zeta/d$。随后，我们讨论以下情形：

The last term on the right-side of Eq. (1.8) is a d-independent, d-dimensional mean-field approximation of the active stress, where δ_{ij} is the Kronecker tensor. The S term is not affecting the linear stability of the model, while it takes into account that an active particle can act as pusher ($\zeta<0$) like *E. coli*[32–34] or *Bacillus subtilis* or as a puller ($\zeta>0$) like *Chlamydomonas reinhardtii*.[32,35] Finally, λ_0 and λ_1 in Eq. (1.7b) are equal to $\lambda_0 = 1-\zeta$ and $\lambda_1 = -\zeta/d$. Subsequently, we discuss the following cases:

- 对于 $\eta_0 > 0$ 且 A、C 和 η_2 为零时，式(1.7b)简化为被动流体的标准纳维-斯托克斯方程(1.1a)。
  For $\eta_0 > 0$ and A, C, and η_2, Eq. (1.7b) reduces to the standard Navier-Stokes equation (1.1a) for a passive fluid.
- 对于 $\eta_0 \geqslant 0$ 且 $\eta_2 = 0$，式(1.7b)简化为经典 Toner-Tu 模型的不可压缩形式[25–27]。
  For $\eta_0 \geqslant 0$ and $\eta_2 = 0$, Eq. (1.7b) reduces to an incompressible version of the classical Toner–Tu model.[25–27]
- 对于 $\eta_0 < 0$ 且 $\eta_2 > 0$，式(1.7b)提供了对稠密细菌悬浮液中观测到的湍流介观尺度不稳定性的最简单通用连续介质描述[24]。
  For $\eta_0 < 0$ and $\eta_2 > 0$, Eq. (1.7b) provides a simplest generic continuum description of the mesoscale turbulent instabilities observed in dense bacterial suspensions.[24]

关于活性湍流的更多细节见第 2a 章。
Further details on active turbulence are provided in Chapter ??.

1.2 活性流体流变测量与灵敏度问题 Rheometry of active fluids and the problem of sensitivity

活性流体的流变响应通常是非线性的；对于推型游动体（$S<0$）悬浮液，可以观察到类超流体状态（第1.3节），因此，这些细菌悬浮液通常是“低黏度流体”，其零剪切黏度为 $\lim_{\dot\gamma\to 0}\eta(\dot\gamma) = \eta_0 \leq 1$ mPa·s，其中 $\dot\gamma$ 为剪切速率[19,34,36]。为表征低黏度流体，常规（旋转式）流变仪需要配备能最大限度提高仪器灵敏度的流动几何结构。本节简要介绍常见的测量几何结构（因为下文将比较使用不同几何结构的多种仪器所获得的数据，锥板几何，见图 (1.1)A，其中测量工具是

The rheological response of active fluids is usually non-linear and for pusher ($\zeta<0$) suspensions, a superfluid-like regime can be observed (Section 1.3). Therefore these bacterial suspensions are usually "low viscosity fluids", with a zero-shear viscosity $\lim_{\dot\gamma\to 0}\eta(\dot\gamma) = \eta_0 \leq 1$ mPa·s, where $\dot\gamma$ is the shear rate[19,34,36]. To characterize low viscosity fluids, conventional (rotational) rheometers need to be equipped with flow geometries that maximize the instrument sensitivity. A short overview of common measuring geometries is provided in this section since in the following paragraphs data coming from several instruments equipped with different geometries are compared. The cone-plate geometry, Fig. (1.1)A, in which the measuring tool is

截锥，其锥角α小于2°（出于解析方面的考虑），可在间隙中产生均匀的$\dot{\gamma}$，适用于粒径最大约为1微米。图（1.1）B为经典的同轴圆筒测量单元，也称为Taylor-Couette，由半径为R_1的外圆筒（“杯体”）、半径为R_2，长度为L_H的同轴内圆筒（“转子”）以及两圆筒之间的小间隙H组成，由此形成较简单的流场。为提高灵敏度，通常选用双壁库埃特几何，其示意图见图（1.1）C。在双壁几何中，样品装载在下部（“杯体”）和上部（“转子”）工具之间的空间内。杯体与驱动电机相连，电机施加角速度w，而转子连接到测量扭矩L的力传感器。参照图1，壁面处的名义剪切速率γ与w的关系为

a truncated cone with an angle α below 2° for analytical reasons, provides an homogeneous $\dot{\gamma}$ in the gap, and is recommended for suspensions with particle sizes up to approximately 1 μm. Fig. (1.1)B is the classical coaxial cylinder cell, also known as "Taylor-Couette", consisting of an outer cylinder ("cup") of radius R_1, a coaxial inner cylinder ("bob") of radius R_2, length L_H, and a small gap, H, between the cylinders, resulting in a simpler flow field. To increase sensitivity a typical choice is the double-wall Couette geometry, which is schematically shown in Fig. (1.1)C. In the double-wall geometry, the sample is loaded in the space between the lower ("cup") and the upper ("bob") tools. The cup is connected to a machine motor, which imposes an angular velocity ω, while the bob is connected to a force transducer which measures the torque **L**. With reference to the Figure 1.1, the nominal shear rate at the walls $\dot{\gamma}$, is related to ω, by

$$\dot{\gamma} = \omega \left[\frac{1}{\left(\frac{R_2}{R_1}\right)^2 - 1} + \frac{1}{1 - \left(\frac{R_3}{R_4}\right)^2} \right], \tag{1.9}$$

而L is 与表观平均剪切应力σ相关，其关系为

while L is related to the apparent, averaged shear stress $\overline{\sigma}$ by

$$L = \sigma_1 2\pi R_2^2 L_H + \sigma_2 2\pi R_3^2 L_H = \overline{\sigma} 2\pi L_H \left(R_2^2 + R_3^2\right), \tag{1.10}$$

with σ_1 and σ_2 being the shear stress on the inner and outer bob surface respectively. Finally, the apparent shear viscosity η_{app} is readily obtained as

$$\eta_{app} = \frac{\overline{\sigma}}{\dot{\gamma}}. \tag{1.11}$$

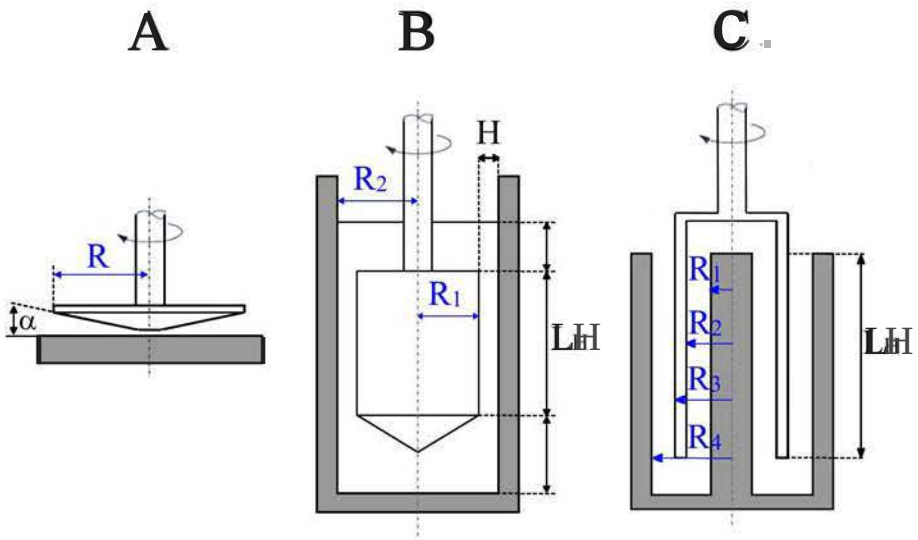

图1.1：几何示意图：（A）锥板几何；（B）Taylor-Couette几何；（C）双壁库埃特几何。对于所有这些几何结构，仪器的一部分固定，另一部分绕其轴线旋转（图中的虚线）。

Figure 1.1: Schematic diagrams of (A) cone-plate geometry, (B) Taylor-Couette geometry, (C) double-wall Couette geometry. Each of all geometries, one part of the rotates around its axis (dashed lines in the figure).

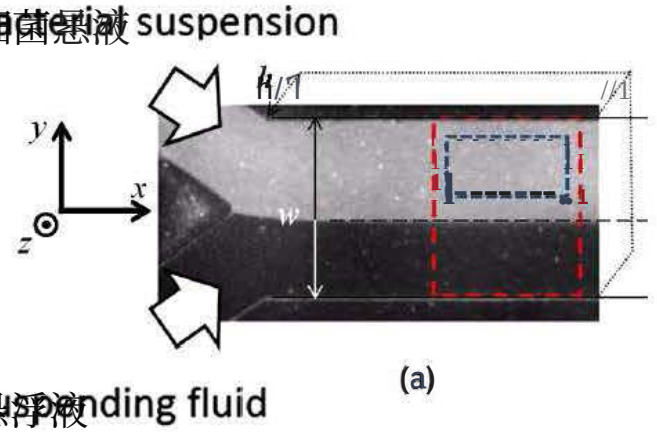

图 1.2 Gachelin 等人[36]细菌悬液通过荧光示踪粒子进行可视化，细菌悬液和缓冲液的流量 Q 均由注射泵控制。表观黏度比 η_{app}/η_s 根据两股流体流束宽度之比 d_1/d_0 估算，即 $\eta_{app}/\eta_s = d_1/d_0$。[37] 经许可转载自文献 Ref. [36]，并经[美国物理学会]许可。版权所有 [2013]。

Figure 1.2 The experimental setup used by Gachelin *et al.*[36] The bacterial suspension is visualized by means of fluorescent seeding beads. The flow rate Q of both the bacterial suspension and the buffer are controlled by a syringe pump. The viscosity ratio η_{app}/η_s is estimated from the ratio between the widths of the two streams d_1/d_0 as $\eta_{app}/\eta_s = d_1/d_0$.[37] Reproduced from Ref.[36] with permission from [American Physical Society], Copyright [2013].

推型游动微生物悬浮液的 η_{app} 可低至缓冲介质（溶剂）黏度 η_s 的 20%，这一情况出现在 0.01 s^{-1} ≤ $\dot{\gamma}$ ≤ 1 s^{-1} 的剪切速率范围内。即使使用灵敏度很高的测量仪器，例如配有双壁库埃特[Couette]几何结构（圆柱形库埃特）的 ARES-G2 流变仪，相应扭矩 M 也只有 10^{-4} μN·m ≤ M ≤ 10^{-2} μN·m，低于仪器可测量的最小值 M_{min} = 0.1 μN·m，[38] 因此会导致数据不准确。为克服这一技术难题，34,39 可使用配有反向旋转工具的 Contraves 30 库埃特流变仪，应能够可靠地测量低黏度流体，剪切速率低至 10^{-6} s^{-1}，[40] 此外，Gachelin *et al.*[36] 使用微流体装置对细菌悬液进行测量，[37] 固定 η_{app}/η_s 比值，误差小于 10%，从而避开旋转流变仪所面临的灵敏度问题。

The η_{app} of pusher suspensions can become as low as 20% of the buffer viscosity η_s over a range of shear rates $0.01\ s^{-1} \leq \dot{\gamma} \leq 1\ s^{-1}$.[34] Even in cases of very sensitive measurement apparatus such as the ARES-G2 rheometer equipped with a double wall Couette geometry (cylindrical Couette), the corresponding values of the torque M would be 10^{-4} μN·m ≤ M ≤ 10^{-2} μN·m, which is below the minimum value measurable by the instrument, M_{min} = 0.1 μN·m,[38] i.e., leading to inaccurate data. In order to overcome such technical difficulty, a Contraves 30 Couette rheometer equipped with a counter-rotation tool, which provides reliable measurements for low viscosity fluids in shear rates down to 10^{-6} s^{-1},[40] was used. Moreover, Gachelin *et al.*[36] used a microfluidic Hele-Shaw cell,[37] Fig. 1.2, which allows to determine the η_{app}/η_s ratio directly from flow visualization experiments, with an error smaller than 10%, thus circumventing the sensitivity issues encountered by rotational rheometers.

1.3 悬浮液的表观黏度 The apparent viscosity of active particle suspensions

对活性流体动力学的分析使 Hatwalne 等人[41]预测，在牛顿基质中存在推型游动体会使悬浮液的体相黏度低于缓冲液，而拉型藻类则会使黏度升高。Sokolov 和 Aranson[42]随后通过测量悬浮液中一种推型物种（枯草芽孢杆菌细胞）的剪切黏度，实验证实了这一点。[42] 与非运动细胞悬浮液相比，枯草芽孢杆菌细胞悬浮液的剪切黏度最多降低了 7 倍。为解释这一效应，Saintillan 提出了一种流动曲线预测动力学模型，用于描述低雷诺数下无界稀悬浮液中的无扭矩粒子。[43]

The analysis of the active fluid dynamics led Hatwalne *et al.*[41] to predict that the presence of pushers in a Newtonian matrix would lower the bulk viscosity of the suspension with respect to that of buffer, while puller algae would act to increase the viscosity.[41] This was experimentally demonstrated in the work by Sokolov and Aranson focusing on shear viscosity measurements of a pusher species (*Bacillus subtilis* cells) in a suspension.[42] The shear viscosity of the *Bacillus subtilis* cells suspension was reduced up to 7 times compared to suspensions of non-motile cells. To explain such an effect, Saintillan proposed a flow curve predictive kinetic model for unbounded dilute suspensions of torque-free particles at low Reynolds number.[43]

The configuration of the suspension is characterized by the particle orientation distribution,

配置——悬浮液的构型由粒子取向分布

$\psi(\mathbf{p},t)$ is the particle orientation distribution function, which satisfies the Fokker–Planck equation including the effects of the external shear flow, rotational diffusion, and particle tumbling. In this model, it is assumed that the suspension is homogeneous in space, which is a valid approximation in the limit of infinite dilution, i.e., the inter-particle hydrodynamic interactions are neglected. As a matter of fact, active particle simulations have shown that at low volume fractions swimming particles undergo ballistic motions for most of the time, except for rare particle-particle encounters during which their orientations change, resulting in an effective rotational diffusion over long times, i.e., the single-cell rotational diffusion d_r can be used to model hydrodynamic diffusion.[44–46] The evolution equation for $\psi(\mathbf{p},t)$ is then

$\psi(\mathbf{p},t)$ 表征粒子指向矢 $\mathbf{p}$ 的概率分布函数，它满足含有流场、旋转扩散和粒子翻滚效应的 Fokker–Planck 方程。该方程包含外部剪切流、转动扩散和粒子翻滚的影响。在此模型中，假设悬浮液在空间中是均匀的，在无限稀释极限下，这是一个有效近似，即忽略粒子间的流体动力学相互作用。事实上，活性粒子模拟表明，在低体积分数下，游动粒子大部分时间都进行弹道运动，只有在罕见的粒子间碰撞过程中，其取向才会发生变化，从而在长时间尺度上产生有效的转动扩散，即可以用单细胞转动扩散 d_r 来模拟流体动力学扩散。[44–46] 于是，$\psi(\mathbf{p},t)$ 的演化方程为

$$\frac{\partial \psi}{\partial t} + \nabla_p \cdot (\dot{\mathbf{p}}\psi) - d_r \nabla_p^2 \psi + \frac{1}{\tau_r}\left(\psi - \frac{1}{4\pi}\right) = 0 \tag{1.12}$$

where ∇_p is the gradient operator on the surface of the unit sphere, and τ_r is the rotation time between tumbling events.[44–46] Knowledge of $\psi(\mathbf{p},t)$ allows the direct evaluation of the relative viscosity as expressed by Saintillan[19]

其中，∇_p 是单位球面上的梯度算子，τ_r 是翻滚事件之间的特征时间。[44–46] 已知 $\psi(\mathbf{p},t)$ 即可直接求得 Saintillan[19] 所表达的相对黏度

$$\frac{\eta_{app}}{\eta_s} = 1 + \frac{\pi n \ell^3}{6\ln(2\ell/d)}\left\langle p_x^2 p_y^2 \right\rangle + \frac{3nk_BT}{\eta_s \dot{\gamma}}\left\langle p_x p_y \right\rangle + \frac{n\zeta}{\eta_s \dot{\gamma}}\left\langle p_x p_y \right\rangle \tag{1.13}$$

where η_{app} denotes the apparent viscosity, i.e., the ratio between shear stress and shear rate, η_s is the solvent viscosity, n is the particle number density, ℓ and d are the length and thickness of the rod, ζ is the strength of the swimming stresslet, k_B is the Boltzmann constant and T is the temperature. The three terms of Eq. (1.13) results from flow-induced, Brownian and active stress, respectively. In the weak-flow limit, i.e., $\dot{\gamma}/d_r \to 0$, where d_r is the rotational diffusion and in the case of smooth swimmers (i.e., tumbling correlation time, $\tau_r \to \infty$) then $\langle p_x^2 p_y^2 \rangle \to 1/15$ and $\langle p_x p_y \rangle \to \beta/30 d_r$, where $\beta = ((b/d)^2 - 1)/((b/d)^2 + 1)$ denotes Bretherton's constant which is approximately 1 for a slender swimmer, leading to the low-shear-rate viscosity estimate

其中 η_{app} 为表观黏度，即瞬时剪切应力与剪切速率之比；η_s 是溶剂黏度；n 和 ℓ、d 分别是杆的数密度、长度和厚度；ζ 是游动应力偶极子的强度，k_B 是玻尔兹曼常数，T 是温度。式 (1.13) 中的三项分别源于流动诱导应力、布朗应力和活性应力。在弱流极限下，即 $\dot{\gamma}/d_r \to 0$，其中 d_r 为转动扩散；对于平滑游动体（即翻滚相关时间 $\tau_r \to \infty$），则有 $\langle p_x^2 p_y^2 \rangle \to 1/15$ 和 $\langle p_x p_y \rangle \to \beta/30 d_r$，其中 $\beta = ((b/d)^2 - 1)/((b/d)^2 + 1)$ 表示 Bretherton 常数，对于细长游动体，该常数约为 1，由此得到低剪切速率黏度估值

$$\lim_{\dot{\gamma}\to 0} \frac{\eta_{app}}{\eta_s} = 1 + \frac{\pi n \ell^3}{30\ln(2\ell/d)}\left[\left(\beta + \frac{1}{3}\right) + \left(\beta\frac{\zeta}{k_BT}\right)\right]. \tag{1.14}$$

Eq. (1.14) expresses solvent viscosity (first term), zero-shear-rate particle contribution to the viscosity in a suspension of passive rods (second term), and the effect of active swimmers involving the swimming stresslet ζ (third term). A characteristic time for swimming t_c; i.e., the time for a swimming particle to drag fluid along is length under the effect of its permanent force dipole can be defined[43]

式 (1.14) 表示溶剂黏度（第一项）、被动杆状粒子悬浮液中零剪切速率下的粒子黏度贡献（第二项），以及涉及游动应力偶极子的活性粒子效应（第三项）。可以定义游动特征时间 t_c，即游动粒子在其永久力偶极子的作用下拖曳流体经过自身长度所需的时间：[43]

$$t_c \equiv \frac{\pi \eta_s \ell^3}{6|\zeta|\ln(2\ell/d)}, \tag{1.15}$$

Fig. 1.13 reports Saintillan's[43] kinetic model at several t_c values, i.e., at several values of the particle activity, along with experimental values for pusher and puller suspensions. The model

图 1.13 展示了 Saintillan[43] 动力学模型在多个 t_c 值下的结果，即在多个粒子活性下的结果，同时还展示了拉型游动体和推型游动体悬浮液的实验值。该模型

能够完美预测 Lopez 等人使用 Taylor-Couette 几何结构对推力型大肠杆菌游动微生物进行实验所得的数据。[34] 这些微生物的细菌体积为 1 微米^3，对应的 d_{rc} 为 0.42，d_r = 2.3 rad^2/s[47,48]，C = 1.9 微米^2，且在体积分数为 0.11% 时为 (−7.98·10^{-19} Nm^{-32})，而在更高体积分数下，黏度下降得更为明显，并遵循卡罗定律。

predicts perfectly the experimental data by Lopez *et al.*[34] obtained using a Taylor-Couette geometry for pushers with a bacterial body volume of 1 μm^3 giving a d_{rc} of 0.42 with d_r = 2.3 rad^2/s[47,48] C = 1.9 μm and ζ = 7.98·10^{-19} Nm[32] at a volume fraction of 0.11%, while at higher volume fractions a more pronounced decrease in the viscosity is observed and it follows the Carreau law.

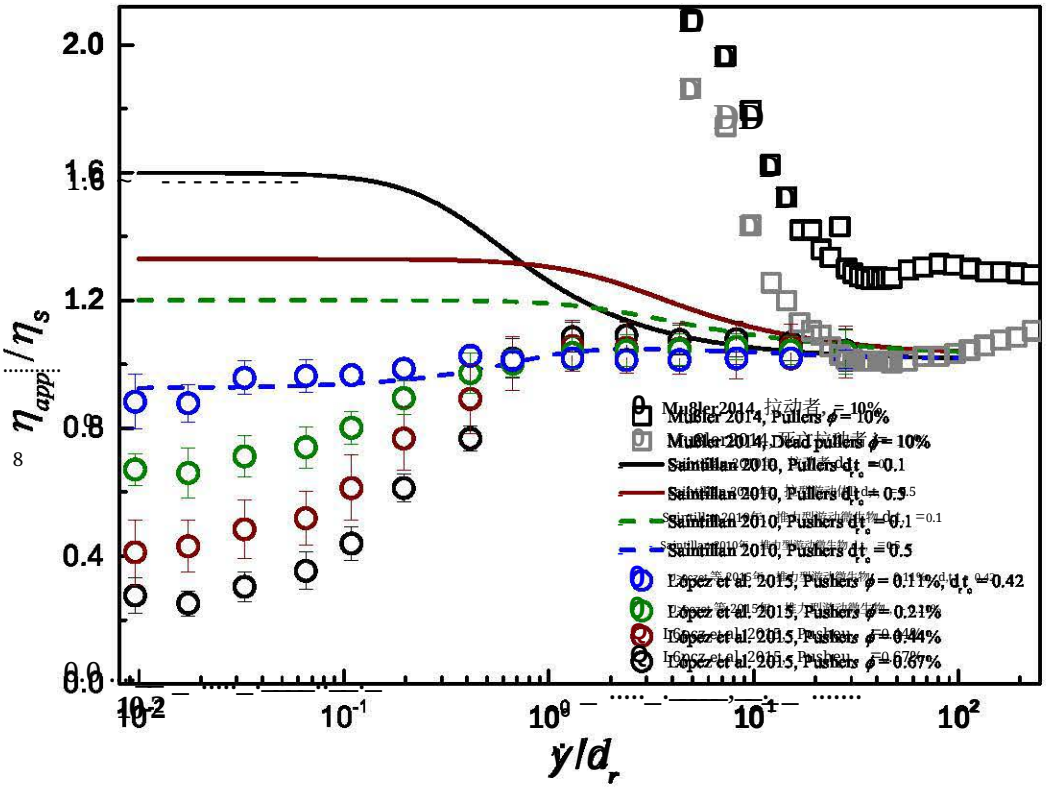

图 1.3 推型游动体和拉动者的悬浮液流动曲线，与 Saintillan 的理论预测进行比较[43]。空心圆：使用泰勒-库埃特装置测得的大肠杆菌悬浮液的约化黏度，测量条件为 0.11% $\leq \phi \leq$ 0.65%。[34] 空心方块：锥板测量显示，死亡（非运动性）拉型游动体的果因衣藻悬浮液约化黏度降低。[49] 实线：Saintillan 模型对稀释的平滑游动体悬浮液所作的预测，该预测随游动时间 t_c 和旋转扩散 d_r 而变化。其中 Bretherton 常数 β = 1，理论预测改编自参考文献[43]，经 [Springer Nature] 许可转载，版权归 [2010] 所有。推力型游动微生物的实验数据改编自参考文献[34]，经 [美国物理学会] 许可转载，版权归 [2015] 所有。拉型游动体的实验数据改编自参考文献[49]，经 [比文作者及导师] 许可转载，版权归 [2014] 所有。

Figure 1.3 Flow curves of suspensions for both pusher and puller swimmers compared with the theoretical prediction by Saintillan[43]. Hollow circles: reduced viscosities of *E. coli* suspensions measured with a Taylor-Couette device at 0.11% $\leq \phi \leq$ 0.65%.[34] Hollow squares: cone-plate measurements of *Chlamydomonas reinhardtii* suspensions showing a decrease in reduced viscosity for the dead (non-motile) pullers.[49] Solid lines: the Saintillan model prediction for dilute suspensions of smooth swimmers as a function of swimming time, t_c, and the rotary diffusion, d_r, where the Bretherton constant β = 1. Theoretical prediction adapted from Ref.[43] with permission from [Springer Nature], Copyright [2010]. Experimental data of pushers adapted from Ref.[34] with permission from [American Physical Society], Copyright [2015]. Experimental data of pullers adapted from Ref.[49] with permission from [the author and supervisor of the thesis], Copyright [2014].

在图 1.3 中，推力型悬浮液的相对黏度随体积分数呈现出相似的趋势：(i) 在极低剪切速率下可观察到活性黏度平台，此时 η_{app} 低于 η_{app}（类超流体状态）；(ii) 在中等剪切速率下出现剪切增稠状态，使 η_{app} 达到接近 η_s；(iii) 在高剪切速率下出现牛顿平台，此时活性黏度贡献可以忽略不计。类超流体状态并不违反热力学原理，因为细菌消耗化学能来平衡。

In Fig. 1.3, the relative viscosity of the pusher suspensions display similar trends with volume fractions: (i) an active viscous plateau is detectable at very low shear rates where η_s is lower than η_{app} (superfluid-like regime); (ii) a shear thickening regime appears at intermediate shear rate values bringing the η_{app} to a value close to η_s; (iii) a Newtonian plateau at high shear rates where the active contribution to viscosity is negligible. The superfluid-like regime is not a violation of thermodynamic principles, since the bacteria consume chemical energy to balance

the viscous dissipation in the flowing suspension, thus allowing for a sustained flow without any applied torque. The Saintillan prediction is made in a very diluted regime, i.e., below the critical volume fraction determined by Martinez et al. et al. as 0.75% for *E. coli*. Above such critical volume fraction, large-scale collective motion emerges from the quiescent state, and the flow becomes nonlinear. Consequently, the apparent viscosity results from a complex interplay between hydrodynamics, particle transport, and hydrodynamic interactions involved in the motion of the suspended active particles as well as the measured gap size (see Section 1.4). Furthermore, the apparent viscosity is also a function of the bacteria aspect ratio, which is considered to be $\ell/d > 6$[53] for filamentous *E. coli* strains. From an experimental viewpoint, it is worth noting that individual cells of a single species of bacterium vary in length during growth in culture leading to $2.31 < \ell/d < 9.31$.[36] The shear-thinning nature of algae suspensions has been reported by Rafai *et al.*[35] and Mussler *et al.*[54] in particular for a suspension of *Chlamydomonas reinhardtii*, a puller microswimmer. Their main findings confirms Hatwalne *et al.*'s prediction, i.e., the viscosity of the active cells suspensions is higher than the viscosity of the same dead cells (non-motile) suspensions as reported by Sokolov and Aranson.[41,42]

图 1.3 展示了采用锥板几何测得的活性和非活性莱茵衣藻*拉氏游动体*悬浮液的流动曲线[54]。作者证明，在所研究的剪切速率区间内，Taylor-Couette 几何与锥板几何所得的数值相近。实验数据显然在低剪切速率下偏离了 Saintillan 的预测。然而，10% 的体积分数高于推定游动体悬浮液的体积分数。至少根据模拟结果，推定游动体不存在临界体积分数[55]。尽管实验表明，藻类相互作用会影响黏度增大，[56] 最后需要指出，考虑到 $\dot{\gamma} = 0.4\ \mathrm{rad/s}$[32] 和 $C = 10$[55] 微米，$\mathrm{Dr}_{\mathrm{crit}}$ 为 ~ 0.03，而 $\langle \dot{\gamma} \rangle = 4.3 \times 10^{-17}\ \mathrm{Nm}$，[57] 因此与 $\mathrm{Dr}_{\mathrm{crit}} = 0.1$ 时模拟得到的曲线相距甚远。剪切变稀行为被归因于细胞相互作用和悬浮液的微观结构变化[56,58]，或高体积分数下悬浮液中高度局部化的黏性耗散[59]。Soulies 等人[58] 报告称，在小球藻悬浮液的剪切变稀区间存在絮团。Cagney 等人[60] 研究了浓度为 $\langle \phi \rangle = 5\%$ 的 *P. chuii* 悬浮液在多种剪切速率下的絮凝现象。低剪切速率下的剪切变稀行为被归因于在 10 s-1 时检测到的絮团，而在更高剪切速率下则未报告絮凝现象。Cagney 等人[60] 还报告称，浓度为 $\langle \phi \rangle = 10\%$ 的三角褐指藻悬浮液表现出剪切变稀行为；然而，Wileman 等人[61] 报告称，浓度介于 $\langle \phi \rangle = 0.5\%$ 和 8% 之间时，悬浮液表现出牛顿流变行为，他们提出，可能存在一个临界体积分数，超过该值，三角褐指藻悬浮液便会呈现非牛顿行为。Cagney *et al.*[60] also reported shear-thinning behaviour at low shear rates has been attributed to the detected flocs at $10\ s^{-1}$, whereas no flocculation was reported at higher shear rates.

1.3.1 表观黏度的浓度依赖性 Concentration dependence of the apparent viscosity

图 1.4 展示了推型游动体和拉型游动体在 0.1% 至 13% 以及 5% 至 18% 范围内的 η_{app}/η_s from 0.1 to 13% and from 5 to 18% for pushers and pullers, respectively. Accurate measurements of pushers dispersions (*E. coli* strains) have been obtained by Lopez *et al.* and Martinez *et al.* using a Taylor-Couette geometry. Other measurements have been obtained by using microfluidic rheometers[36,64] and are in agreement with the ones reported here. The generalized Einstein's equation could be adopted in the diluted regime of pusher particles, even though it was originally developed to describe dilute regime ($\phi < 5\%$) of solid spherical particles,

$$\eta_{app} = \eta_s(1 + [\eta]\phi), \tag{1.16}$$

其中，$[\eta]$ 为本征无量纲黏度，对于固体球形粒子其值等于 5/2；η_s 为溶剂黏度，即是浮介质的黏度。然而，在此处，$[\eta] = K(\tau_r/t_r)$ 34,65,66，其中 τ_r 表征游动体的方向持久性，$K(\tau_r/t_r)$[34,65,66] in which τ_r characterizes the directional persistence of a swimming trajectory, $\tau_r = 1/2d_r$[48], while $K \propto (A - B(\tau_r/t_r))$ where A and B depend on the bacterium shape[66–68]. In this diluted regime the relative viscosity is linearly decreasing with the volume fraction for shear rate between 0.022 and 0.075 s^{-1} (Fig. 1.4A) following Eq. (1.16). Lopez *et al.* reported $[\eta] \approx -120$ for ATCC9637 strain with low content of O_2 (empty circles) and $[\eta] \approx -200$ for ATCC9637 strain with high content of O_2 and L-serine (grey circles) and $[\eta] \approx -260$ for RP437 strain with high content of O_2 and L-serine (black circles) using Martinez *et al.*[39] data $[\eta] \approx -150$ for AB1157 strain with a motility buffer. The intrinsic viscosity is a function of both the culture strain and the mobility buffer. In all cases, the active plateau viscosity becomes independent of the volume fraction from 0.75% up to 2.4%. Moreover, in the presence of O_2 and L-serine the local viscous dissipation is macroscopically compensated by the swimming activity, i.e., the viscous response reaches zero.

Mussler *et al.*[54] reported accurate viscosity measurements on *Chlamydomonas reinhardtii* pullers dispersions using a cone-plate geometry in a wide range of volume fraction. Fig. 1.4B adopting the very well-known Krieger-Dougherty model[59]

$$\eta_{app} = \eta_s\left(1 - \frac{\phi}{\phi_{max}}\right)^{-[\eta]\phi_{max}} \tag{1.17}$$

其中 ϕ_{max} 是大堆积分数，对于随机密堆积，其值约为 0.64[69]。然而，克里格-多尔蒂方程可能无法描述最高体积分数下的数据。Cagney 等人[60] 证明，拉动者的体积分数对流变学的影响程度取决于应变率，在低应变率下，流变学强烈依赖于细胞体积分数。这一证据表明，悬浮细胞影响流体流变学的物理机制发生了变化。Cagney 等人[60] 认为，这与低剪切速率下絮团的出现有关，因为形成絮团的趋势会导致观测黏度显著增加。

1.4 浓缩体系与湍流起始 Concentrated Systems and the Onset of Turbulence

作为型游动微生物悬浮液流变学最重要的特征之一，是在体积分数 ϕ 高于 $\phi = 0.75\%$ 时观察到的转变。高于 ϕ 时，该系统会变成一种“超级流体体”，

One of the most important features of the suspension rheology of pushers is the transition observed at volume fractions ϕ above $\phi = 0.75\%$. Above ϕ, the system becomes a “super-fluid”,

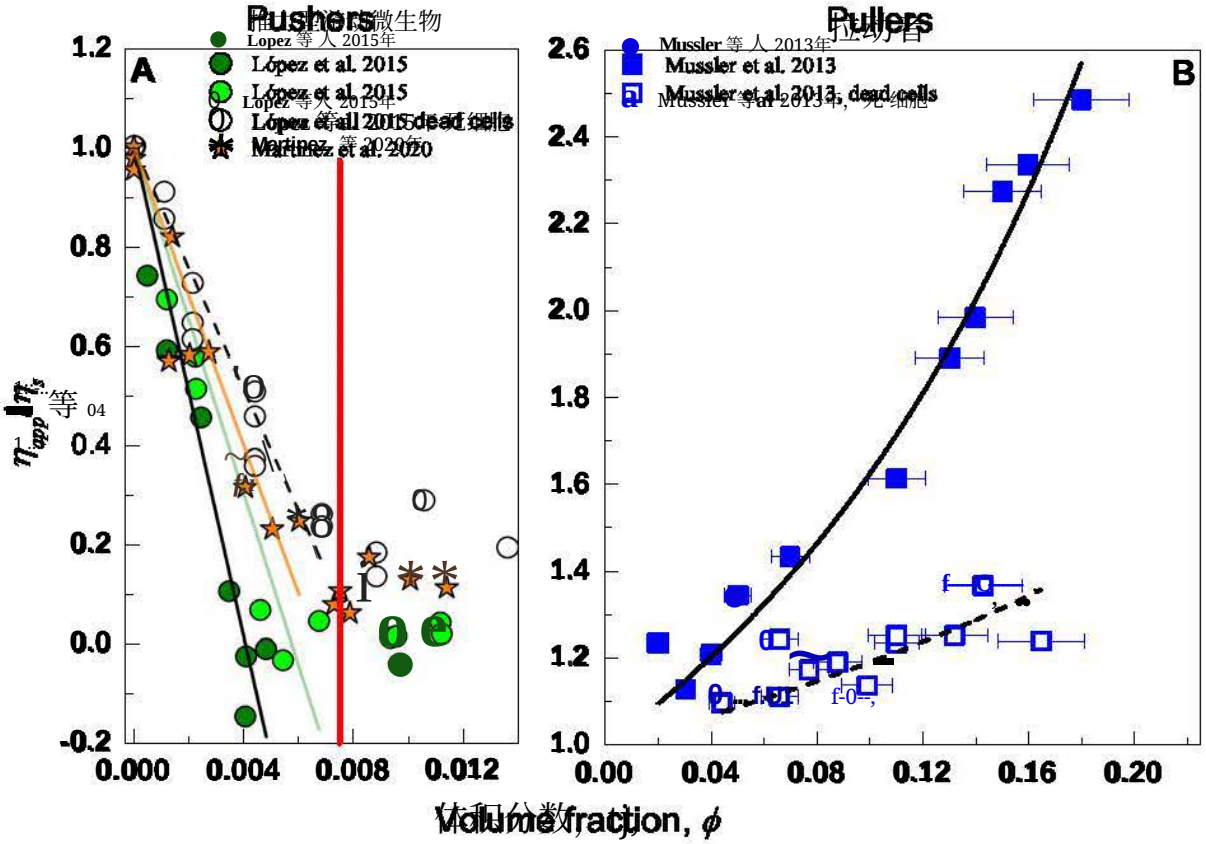

图1.4: 推力型游动微生物（A）和拉动者（B）的相对黏度随体积分数的变化。A：使用Taylor-Couette装置对大肠杆菌悬浮液进行测量，结果显示，随着体积分数增加，η_{app}/η_s 逐渐衰减至零。A面板中的实线为线性拟合。B：使用锥板几何测量的莱茵衣藻悬浮液相对黏度随体积分数的变化。[54] B面板中的实线为Krieger-Dougherty拟合，即公式1.16，其中 ϕ_{max} = 0.63和0.64，$[\eta]$ = 4.40和0.64，$[\eta]$ = 4.40和1.60。推型游动体的实验数据改编自文献[34]，经[美国物理学会]，许可。版权所有[2015]。推型游动体的实验数据改编自文献[39]，公开数据。拉型游动体的实验数据改编自文献[54]，经[IOP Publishing]，许可。版权所有[2013]。

Figure 1.4: Relative viscosity as a function of volume fraction for pushers (A) and pullers (B). A: measurements of *E. coli* suspensions performed with a Taylor-Couette device showing that η_{app}/η_s decays towards zero with increasing volume fraction. The solid lines in panel A are linear fittings. B: relative viscosity of *Chlamydomonas reinhardtii* suspensions measured in a cone-plate geometry as a function of the volume fraction.[54] The solid lines in the panel B are Krieger-Dougherty fittings, Eq. 1.16, in which ϕ_{max} = 0.63 and 0.64 and $[\eta]$ = 4.40 and 0.64, for $[\eta]$ = 4.40 and 1.46 and 1.60. Experimental data of pushers adapted from Ref.[34] with permission from [American Physical Society], Copyright [2015]. Experimental data of pushers adapted from Ref.[39] public data. Experimental data of pullers adapted from Ref.[54] with permission from [IOP Publishing], Copyright [2013].

也就是说，测得的宏观剪切黏度变得可以忽略不计，流场则变为非线性。[39]

Le, the measured macroscopic shear viscosity becomes negligible, and the flow field becomes non-linear.[39]

Guo *et al.*[70] studied the velocity field of *E. Coli* suspensions under different shear rate conditions, the velocity gradient concentrates within the bulk of the flow, so that a boundary layer h_s near the top and the bottom of the flow geometry is formed, where the velocity gradient is negligible. For volume fractions lower than 0.01 approximately, the non-linearity of the velocity profile disappears (see Fig. 1.5).

Guo *et al.*[70] 研究了在不同剪切速率振幅下大肠杆菌悬浮液的速度场 1I 使用由两块相距边间隙的 θ 极组成的平面振荡剪切装置，H，即施加振荡剪切流。关键结果是，在弱剪切条件下，速度梯度集中于流动主体内部，因此在 h_s 顶部和底部附近的流动几何区域形成边界层，其中速度梯度可忽略不计。当体积分数约低于0.01时，速度剖面的非线性消失（见图1.5）。

作者根据速度测量提取了细菌群游所产生流动的涡量平方积分，[71] $\Omega_y = \langle W_y/2 \rangle$ 其中 $\partial_x u_z - \partial_z u_x$ 为平面内涡量 $\omega_y/2$，有趣的是，

The authors extracted the enstrophy of the flow due to bacterial swarming from the velocity measurements,[71] $\Omega_y = \langle \omega_y/2 \rangle$ where $\partial_x u_z - \partial_z u_x$ is the in-plane vorticity. Interestingly, the

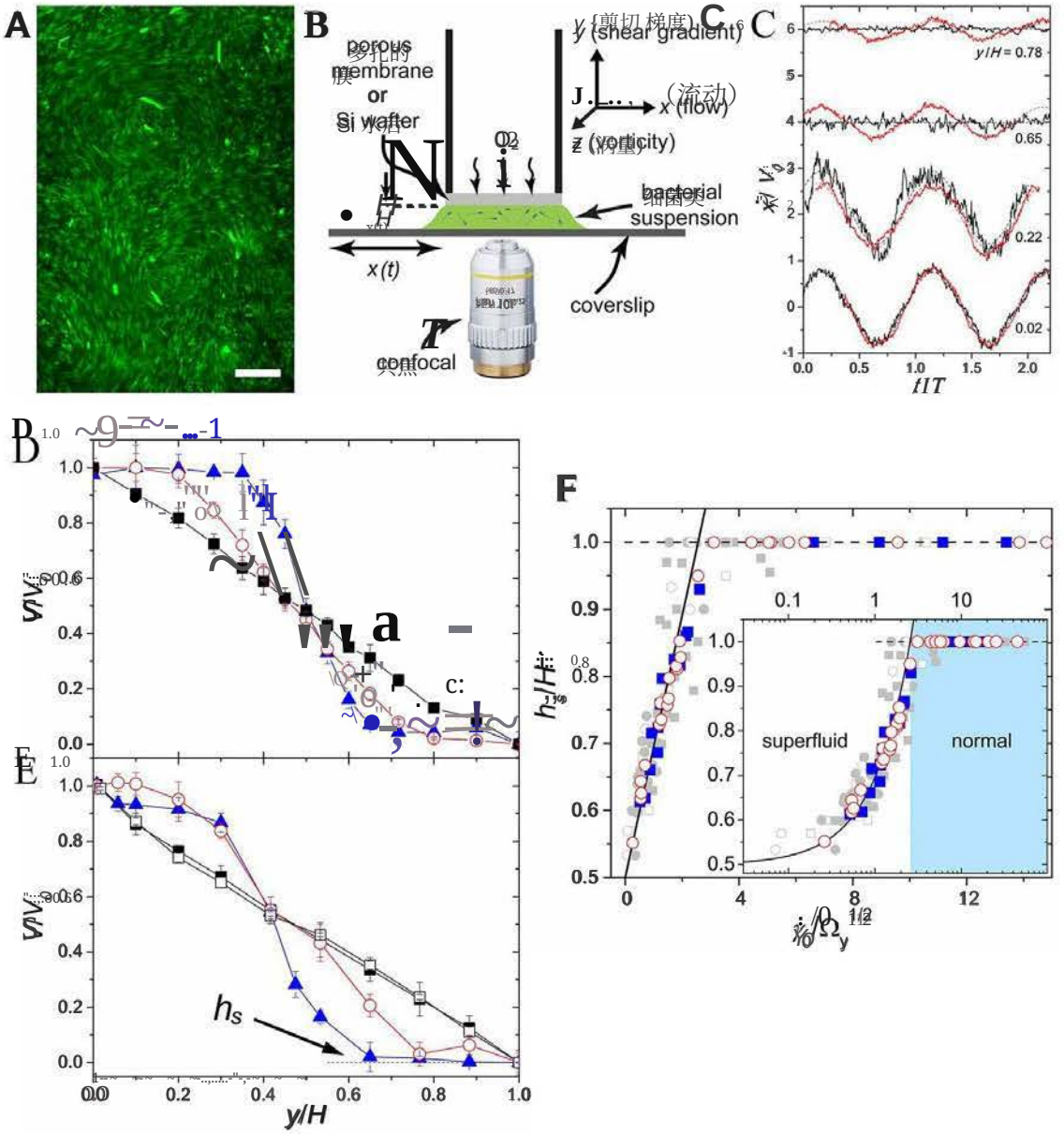

图1.5：细菌群游导致的剪切带形成：（A）细菌群游的一个示例；（B）流动可视化的实验装置；（C）不同 y/H，条件下速度的时间变化；（D）固定细菌浓度下剪切速率对速度剖面的影响；（E）在 $\dot{\gamma}_0 = 0.16$ s^{-1} 和 $n = 10n_0$（黑色方块）、$n = 40n_0$（红色圆圈）和 $n = 50n_0$（蓝色三角形）条件下的归化剪切剖面，其中 $n_0 \sim 8\cdot10^8$ mL^{-1}。图1.5F：无量纲边界层宽度 h_s/H 随 y_0/Q_y 的变化图，展示剪切带形成行为的普适性。经许可改编自参考文献[1]，获[美国国家科学院]，许可，版权所有 [2018]。

Figure 1.5: Shear banding due to bacterial swarming: (A) an example of bacterial swarming; (B) the experimental setup for flow visualization; (C) temporal variation of velocity for different y/H; (D) effect of shear rate on the velocity profile for a fixed bacterial concentration $n = 50n_0$ and $\dot{\gamma}_0 = 0.42$ s^{-1} (black squares), 0.16 s^{-1} (red circles) and 0.055 s^{-1} (blue triangles). (E) Normalised shear profiles at $\dot{\gamma}_0 = 0.16$ s^{-1} and $n = 10n_0$ (black squares), $n = 40n_0$ (red circles) and $n = 50n_0$ (blue triangles) with $n_0 \approx 8\cdot10^8$ mL^{-1}. Fig. 1.5F: the width of the non-dimensionalised boundary layer h_s/H plotted vs γ_0/Ω_y to display the universality of the shear banding behaviour. Adapted from Ref. [1] with permission from [National Academy of Sciences], Copyright [2018].

测量了 h_s 与 $\Omega_y/\dot{\gamma}_0$ 在不同 H_r 条件下的结果，并叠加在同一条曲线上。基于先前提出的活性液体模型，该模型指出剪切速率应与非单调性、[72] 作者提出了一个唯象模型，用于描述 h_s 对 $\dot{\gamma}_0$ 的依赖关系，

measurements of h_s vs. $\Omega_y/\dot{\gamma}_0$ conducted at various H overlapped on the same curve. Based on a previous model of active fluids suggesting the non-monotonicity of the shear-stress versus shear-rate,[72] the authors proposed a phenomenological model for h_s dependence on $\dot{\gamma}_0$,

$$\frac{h_s}{H} = \begin{cases} \frac{1}{2}\left(1 + \frac{\dot{\gamma}_0}{C\sqrt{2\Omega_y}}\right) & \text{if } \dot{\gamma}_0/\sqrt{\Omega_y} \le C\sqrt{2} \\ 1 & \text{if } \dot{\gamma}_0/\sqrt{\Omega_y} \ge C\sqrt{2} \end{cases} \tag{1.18}$$

其中 C 是一个数量级为 1 的常数。该方程与实验观测结果吻合良好。根据对 $\mathbf{u}$ 的测量，速度空间相关性定义为

where C is a constant of order unity. The equation is in good agreement with the experimental observations. From the measurements of $\mathbf{u}$, the velocity-velocity spatial correlation is defined as

$$C_v(r) = \frac{\int\int d\mathbf{r}_i d\mathbf{r}_j \left(\mathbf{u}\left(\mathbf{r}_i\right)\right) \delta\left(r_{ij} - r\right)}{\int d\mathbf{r}_i \left(\mathbf{u}\left(\mathbf{r}_i\right) \cdot \mathbf{u}\left(\mathbf{r}_i\right)\right)}, \tag{1.19}$$

其中 r 是位置矢量，关联长度 ℓ_c 定义为 C_v 等于 $1/e$ 时对应的距离。ℓ_c 在 H 较小时随间隙高度近似线性增加，随后趋于平台，但随细菌浓度变化不大。Guo 等人[39] 的结果清楚表明，受限空间对于调节推型溶液的超流动性至关重要。

where r is the position vector and the correlation length, ℓ_c, is defined as the distance at which C_v becomes equal to $1/e$. The ℓ_c varies approximately linearly with the gap height for small values of H before leveling up to a plateau, but does not change very much with bacterial concentration. The results by Guo *et al.*[39] clearly indicate the importance of confinement in modulating the super-fluidity of pusher solutions.

Martinez 等人[39] 在锥板几何结构中观察了多种 *E. Coli* 悬浮液在固定 $H = 170$ 微米（和体积分数（见图 1.1 B）$\phi \approx 1.7$ 时的流动（见图 1.1 B）。作者将其结果与基于连续介质动力学理论、针对不稳定流动起始条件的临界体积分数预测值进行了比较，[73,74]

Martinez *et al.*[39] visualized the flow of several *E. Coli* suspensions through a cone and plate geometry (fixed $H \approx 170$ microns (see Fig. 1.1 B)). The authors compared their results with a prediction for the critical volume fraction $\phi_c(H, u, \tau_r)$ for the onset of unstable flow based on continuum kinetic theory,[73,74]

$$\frac{\phi_c(H, u, \tau_r)}{\phi_c^{\infty}(400, 15, \tau_r)} \approx 1 + \frac{3}{10}\left(2\pi\frac{u\tau_r}{H}\right) + \frac{1}{5}\left(2\pi\frac{u\tau_r}{H}\right)^2, \tag{1.20}$$

其中，渐近值 $\phi_c^{\infty}(400, 15, \tau_r)$ 是在间隙尺寸为 400 微米、游动速度为 15 微米/秒的计算得到的临界体积分数，$\phi_c(H, u, \tau_r)$ 为 0.75%，而 τ_r 是两次翻滚事件之间的特征时间。有趣的是，方程 1.20 成功预测了实测不稳定流动的起始。在 $\phi_c(H, u, \tau_r)$ 处，速度与 H 的关系曲线从线性变为非线性，而在这一 ϕ 范围内，实测剪切粘度降为零（见图 1.6）。与 Guo 等人的研究类似，[70] 超流动性状态伴随着大型涡旋结构的形成，导致关联长度 ℓ_c 在 $\phi_c(H, u, \tau_r)$ 处从接近零骤增至 >100 微米。

where, the asymptotic $\phi_c^{\infty}(400, 15, \tau_r)$ is the 400 micron gap critical volume fraction at a swimming speed of 15 $\mu m/s$, $\phi_c(H, u, \tau_r) \approx 0.75\%$ and τ_r is the characteristic time between two tumbling events. Interestingly, Eq. 1.20 successfully predicts the onset of the measured unstable flow. At the crossing of $\phi_c(H, u, \tau_r)$, the velocity vs H profiles evolve from linear to non-linear while the measured shear viscosity vanished within the range of ϕ (see Fig. 1.6). Similarly to the work of Guo *et al.*,[70] the superfluid regime is accompanied by the formation of large vortex structures which result in the correlation length, ℓ_c, to suddenly increase from near-zero to >100 μm at the crossing of $\phi_c(H, u, \tau_r)$.

1.5 活性极性液晶流变学 Rheology of active polar liquid crystals

Negro 等人[75] 通过大量格子玻尔兹曼模拟预测了活性极性液晶的流变行为。当活性极性组分与牛顿型被动液体以对称比例混合时，系统会形成层状相，即溶致液晶相。作者研究了极性-被动液晶的相对粘度随活性系数的变化。作者采用了

The rheological behaviour of active polar liquid crystals was predicted by Negro *et al.*[75] by extensive lattice Boltzmann simulations. The system sets, in the lamellar phase, i.e. the polar-isotropic liquid crystalline phase, for the symmetric composition of an active polar component and a Newtonian passive fluid. The authors investigated the behaviour of the relative viscosity of a polar liquid crystal phase as a function of the activity coefficient. The authors adopted the

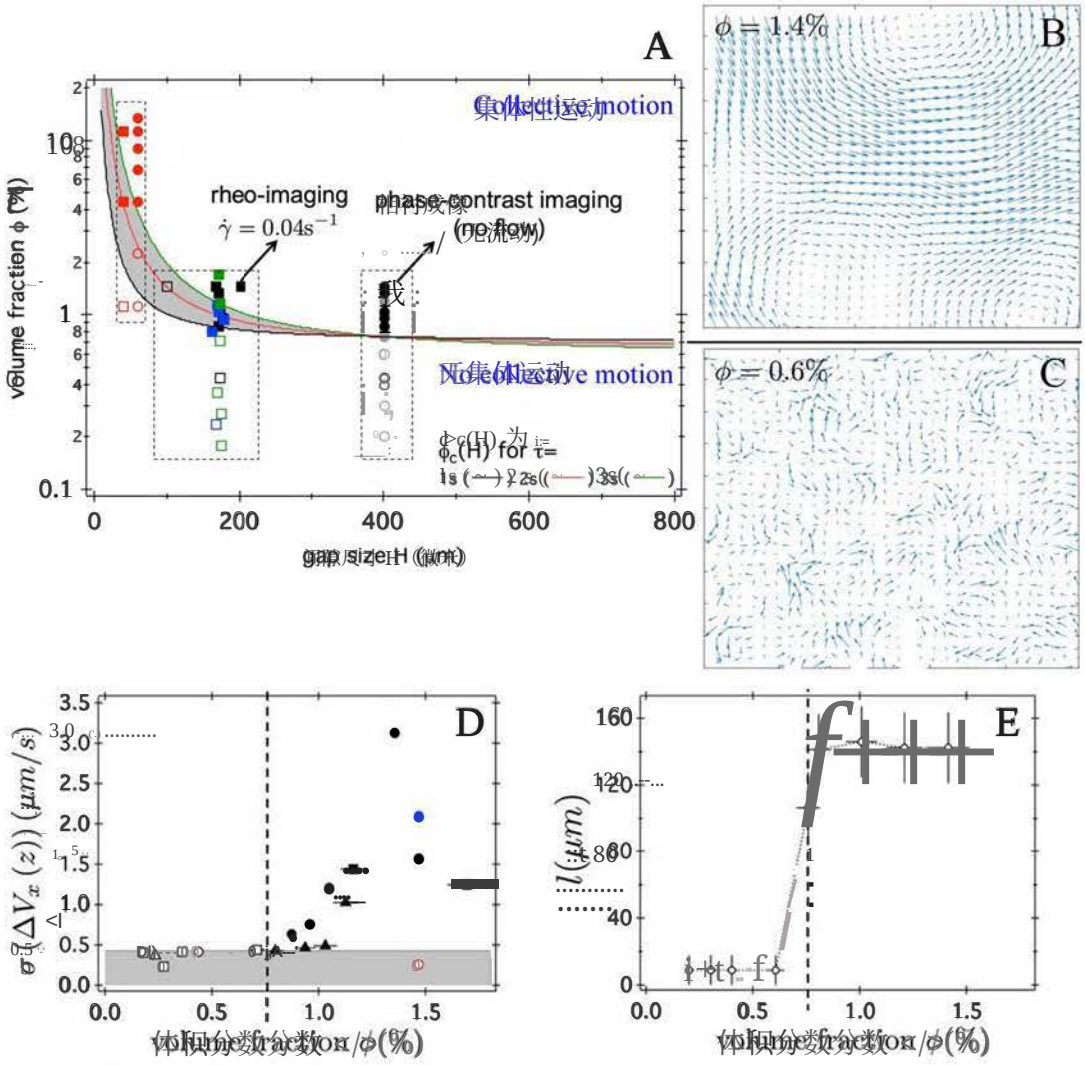

图1.6：推力型游动微生物体积分数 ϕ 和间隙尺寸 H 对观测到的流场的影响。[39]（A）基于 ϕ 和 H 相图中。（B）和（C）：分别展示了个体（A）和集体（B）流动状态下测得的速度场示例。（D）和（E）：速度场的标准差 σ 以及相关长度 l_e 均显著增大，当 $\phi \geq \phi_c = 0.75\%$。图片经授权转载自Martinez 等人。[39]

Figure 1.6: Effects of pushers volume fraction ϕ and gap size H on the observed flow field. [39] (A): ϕ and H phase diagram. (B) and (C): examples of the measured velocity field in the individual (A) and collective (B) flow regimes. (D) and (E): the standard deviation σ and the correlation length ℓ_e of the velocity field are greatly increased for $\phi \geq \phi_c = 0.75\%$. Adapted image courtesy of Martinez *et al.* [39]

埃里克森数 Er，以及活性埃里克森数 Er_a 是用于比较系统中外部剪切流与活性力的相关无量纲量。

$$Er = \frac{\eta \dot{\gamma}}{B}, \tag{1.21}$$

$$Er_a = \frac{\zeta \dot{\gamma}}{B}, \tag{1.22}$$

where B 是层状压缩模量，η 是活性系数。在无剪切系统中，发现层状相会转变为含有运动活性液滴的相，转变发生在 $Er_a \approx 0.11$，正如 Bonelli 等人[76]所预测的那样。当 $Er_a > 1.1$ 时，系统进入混合相，其特征是出现混沌速度模式。[77] 图 1.7A 显示，黏度随活性增强而降低。作者证明，由于层片倾向于与流动方向对齐，层状相区域相较于无剪切系统向更大的 Er_a 值扩展（图 1.7B）。

where B is the lamellar compression modulus and η is activity coefficient. For the shear-free system a transition from the lamellar phase to a phase with moving active droplets is found at $Er_a \approx 0.11$ as predicted by Bonelli *et al.*[76] For $Er_a > 1.1$ the system entered into a mixed phase, characterized by chaotic velocity patterns.[77] Fig. 1.7A shows a decrease in the viscosity with increasing activity. The authors demonstrated that the lamellar phase region is extended towards larger Er_a with respect to the shear-free system due to the tendency of the lamellae to align with the flow 1.7B.

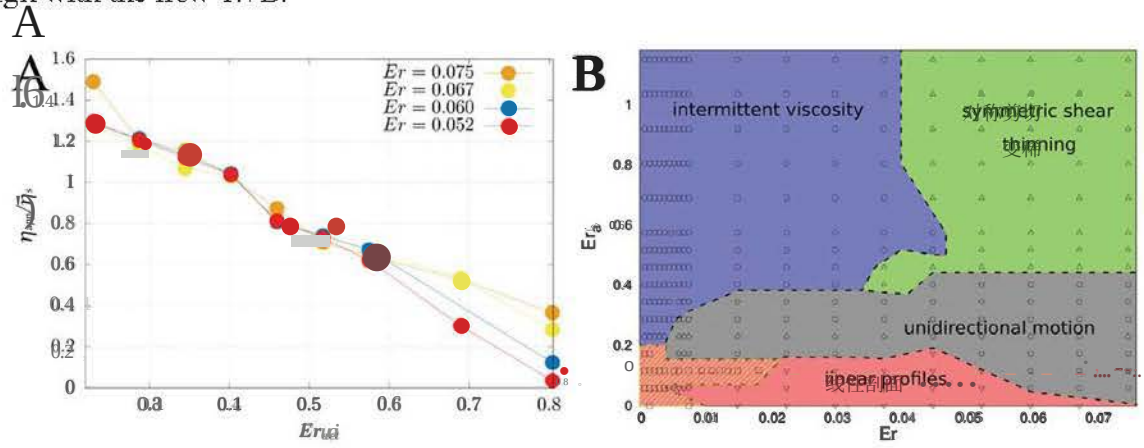

图 1.7：活性极性乳液的相对黏度随活性埃里克森数 Er_a（A）变化，（B）以 Er-Er_a 表示的动态相图。经 [英国皇家化学会] 许可，改编自参考文献[75]，版权[2019]。

Figure 1.7: Relative viscosity of active polar emulsion varying the active Ericksen number Er_a (A). Dynamic phase diagram in terms of Er-Er_a (B). Adapted from Ref.[75] with permission from [RSC], Copyright [2019].

1.6 基质黏弹性影响游动行为 Matrix viscoelasticity affects the swimming behaviour

活性粒子所处的基质对观察到的游动行为起着至关重要的作用。例如，胃液和宫颈液都是黏弹性流体，其中都相思着微生游动体。[78,79] 血液也表现出黏弹性特性，例如其拉伸弛豫时间约为数毫秒。[80] 尽管血液通常是无菌的，但仍可能受到大肠杆菌和革兰氏阳性细菌游动体的感染。[81] 基质的黏弹性会显著改变游动体相对于牛顿情形的行为。游动体所处的大多数基质都可以描述为聚合物溶液，这类流体的特征是具有弛豫时间 A，其范围从毫秒级（

The matrix where active particles are situated plays a crucial role in the observed swimming behaviour. Gastric and cervical fluid, for example, are viscoelastic fluids, and they are both inhabited by microswimmers.[78,79] Blood also exhibits viscoelastic properties such as an extensional relaxation time on the order of a few ms.[80] Even though blood is normally sterile, it can potentially be infected by *E. Coli* and by Gram positive bacterial swimmers.[81] Matrix viscoelasticity can alter significantly the behaviour of swimmers with respect to the Newtonian case. The majority of matrices where swimmers are found can be described as polymer solutions. Such kind of fluids are characterised by a relaxation time λ ranging from milliseconds (in

the inertia regime (of the order of seconds or in the concentrated region.[82–84] Apart from the 在惯性区间（秒数量级或在浓缩区间）[82–84]。因此，除了流数外，主动粒子的运动还会受到德博拉数的影响（见第 1.1 节）；在这一特殊情况下，德博拉数定义为[85]

Reynolds number, the motion of an actively swimming particle will therefore also be affected by the Deborah number (see Section 1.1), which in this special case is defined as[85]

$$\mathcal{D} = \lambda\omega, \tag{1.23}$$

where $\omega = 1/t_o$, is the frequency of flagella rotation. As ω of the swimming bacteria is typically on the order of 20–50 Hz, that of eukaryotic cells is usually lower, leading to a 其中 $\omega = 1/t_o$，是鞭毛旋转的频率。由于游动细菌的 ω 通常约为 20–50 Hz，显然它在许多情况下能够与 20–50 数量级的松弛时间相当。在这种情况下，德博拉数变为 1，导致流体微观结构的非平衡构型。由此产生的重要结果是，即使在 non-equilibrium configuration of the microstructure of the matrix. This has the important consequence that even reciprocal swimming can induce propulsion into a viscoelastic matrix, which constitutes an apparent violation of the "scallop theorem". This was observed first by Lauga,[86] who estimated that the time-averaged speed $\langle U \rangle$ of a swimmer with radius a in a viscoelastic medium descried by the Oldroyd-B model[87] is given by

任意游动也能在黏弹性基质中产生推进，这构成了对“扇贝定理”的表面违反。Lauga 最先观察到这一现象，[86]并估算出，在由 Oldroyd-B模型描述的黏弹性介质中，半径为a的游动体的时间平均速度$\langle U \rangle$为

$$\langle U \rangle = \frac{K a \omega}{1 + \mathcal{D}^2} \left(1 - \frac{\eta_s}{\eta}\right), \tag{1.24}$$

where a is the particle radius, K, 2 and η_s and η are the solvent and the polymer contribution to the overall matrix viscosity. We see that in the limit of $\mathcal{D} \ll 1$, $\langle U \rangle \to 0$ and the "scallop theorem" is recovered. 其中 a 是粒子半径，K，2 和 η_s 以及 η 分别是溶剂和聚合物对基质总黏度的贡献。当 $\mathcal{D} \ll 1$ 时，$\langle U \rangle \to 0$，扇贝定理便得以恢复。

The observations made by Lauga motivated a series of theoretical studies on the locomotion of biological swimmers into viscoelastic media. Keim *et al.*[88] (see Fig. 1.8) demonstrated that asymmetric dimers immersed in a Boger fluid (a constant viscosity, yet elastic) medium are displaced when driven by a time-symmetric magnetic field. The same motion was not observed into a Newtonian medium. The propulsion velocity of the swimmers appeared to depend on the frequency, but not on the amplitude of the applied magnetic field. Qiu *et al.*[89] investigated the behaviour of magnetically activated micro-swimmers in viscoelastic fluids. Lauga 的观察结果促成了多项研究，这些研究探讨了生物游动体在黏弹性介质中的运动。Keim 等[88]（见图 1.8）证明，浸没在 Boger 流体（一种黏度恒定但具有弹性的介质）中的非对称二聚体，在时间对称磁场驱动下会发生位移。在牛顿介质中则未观察到相同的运动。游动体的推进速度似乎取决于频率，但与所施加磁场的振幅无关。Qiu 等[89]研究了磁激活“微型扇贝”在剪切变稀或剪切增稠悬浮介质中的行为，通过调节扇贝张开和闭合阶段的持续时间，作者得以在这两种非牛顿基质中都实现净正位移。

By modulating the duration of opening and closing phases of the scallop, the authors were able to achieve net positive displacement in both the non-Newtonian matrices.

The precise mechanisms which lead to matrix viscoelasticity to alter the swimming of active particles are currently under debate. It has been suggested[47] that the first normal stress difference N_1 observed for polymer solutions and melts in the perpendicular direction with respect to that of shear[85] affects the swimming of cilia and other motor organs of bacteria. Moreover, because the swimming motion curves the streamlines around the bacteria, the flow can also become locally unstable, thus triggering modifications of the particle motion with respect to the Newtonian case. Such transition occurs when the Pakdel-McKinley condition,[90,91] 目前，对于基质黏弹性改变活性粒子游动行为的精确机制仍存在争议。有人提出[47]，聚合物溶液和熔体在垂直于剪切方向上观察到的第一法向应力差 N_1 会影响细菌纤毛及其他运动器官的游动[85]。此外，由于游动运动会使细菌周围的流线弯曲，流动也可能在局部变得不稳定，从而触发对粒子运动的修正，使其相对于牛顿情形发生转变。这种转变发生在 Pakdel-McKinley 条件满足时[90,91]

$$\left[\frac{\lambda_1}{\eta_0}\frac{\langle u \rangle}{R}\sqrt{\frac{N_1}{\tau_{12}}}\right]^{\frac{1}{2}} \geq M_{\mathrm{crit}}, \tag{1.25}$$

satisfies. In Eq. 1.25, η_0 is the zero-shear viscosity, $\langle u \rangle$ is the average speed of fluid, R is the radius of curvature of the streamline, τ_{12} is the shear component of the polymeric stress tensor and M_{crit} is a critical parameter depending on the specific rheological properties of the fluid. 满足条件。在式 1.25 中，η_0 是零剪切黏度，$\langle u \rangle$ 是流体平均速度，R 是流线的曲率半径，τ_{12} 是沿流线方向的剪应力，即聚合物应力张量的剪切分量，M_{crit} 是取决于流体具体流变性质的临界参数。

Patteson *et al.*[47] studied the influence of viscoelasticity of the medium on the swimming and tumbling of *E. coli* bacteria. They used three different polymers and found, as expected, as well as molecular weight. They found that increasing polymer concentration results in an increase of the bacterium velocity and in a reduction of the tumbling frequency. In order to Patteson 等[47]研究了介质的黏弹性对大肠杆菌的游动和翻滚的影响。他们使用了三种不同的聚合物，并如预期所发现，聚合物浓度增加会使细菌速度提高，同时降低翻滚频率。为了

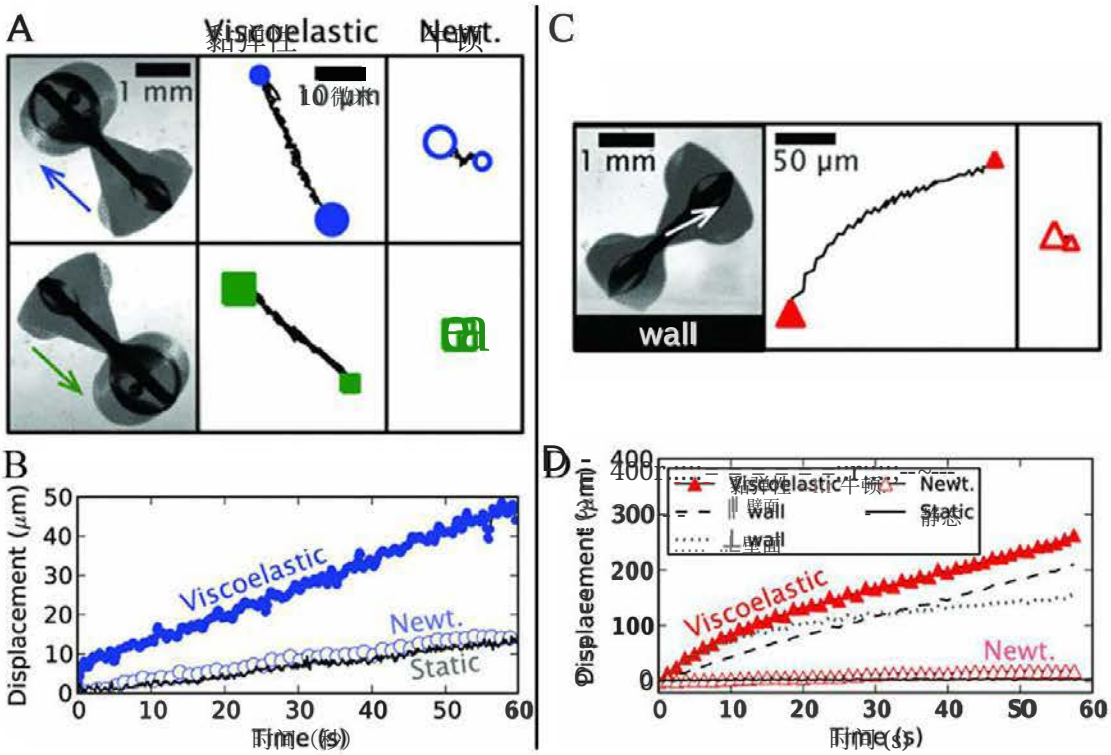

图1.8：基质黏弹性对合成游动体运动的影响。（A）和（B）：加入少量高分子量聚合物。（A）和（B）：adding a small quantity of a high molecular weight polymer induces a net displacement of an asymmetric swimmer at $\mathscr{D} \approx 6$, while no displacement is observed in a Newtonian matrix. （C）和（D）：effects of matrix viscoelasticity on the displacement of an active, synthetic swimmer located near the wall. Adapted from Ref. [88] with permission from [AIP Publishing LLC], Copyright [2012].

解释聚合物导致翻滚减少的原因，作者提出理论认为，聚合物溶液受到剪切时，由于聚合物链被拉伸，会产生法向力 N，进而干扰纤毛运动，导致摆动减少。为了验证这一点，他们在溶液中加入了微量标记DNA。由细菌产生的剪切使构象分布发生变化，从而证实聚合物变形在细菌游动中起着重要作用。

Gagnon *et al.*[92] studied the flow of magnetically-driven bead-rod particles into a wormlike micellar solution for $0.29 \leq \mathscr{D} \leq 29$. At the lowest $\mathscr{D}$, the particles exhibited a small displacement in the direction of the magnetic field. Such displacement increased at $\mathscr{D}=2.9$, and disappeared at the largest $\mathscr{D}$. In order to assess such result, the experiments were coupled with birefringence and velocity measurements to measure local stress and velocity profiles. At intermediate $\mathscr{D}$, striation regions with different values of birefringence were observed near the rod. This indicates the presence of a stress field which caused the observed particle displacement. Rheometric experiments in oscillatory flow demonstrated that the amplitude of the first normal stress difference of the micellar solution at a fixed strain reduced after a few cycles. Because of this, it was proposed that the flow of the asymmetric bead-rod system was driven by a local imbalance of the first normal stress difference N_1.

Han *et al.*[93] investigated the swimming behaviour of micro-scallops made by a variable

前切稀化流体中的游动行为，令人惊讶的是，研究发现，将游动单元的尺寸从4个立方体增至10个立方体，会导致游动方向反转，这归因于游动对象所处局部黏度场的变化。

Gomez-Solano *et al.*[94] studied the dynamics of Janus particles (i. e., synthetic colloids with artificially tuned anisotropic interactions[95]) in a viscoelastic polymer solution. By imputing a laser beam into the system and thereby moving the particles, they observed a dramatic increase of the rotational diffusion, which was related to the viscoelasticity of the medium as well as to the achieved $\mathscr{D} > 1$.

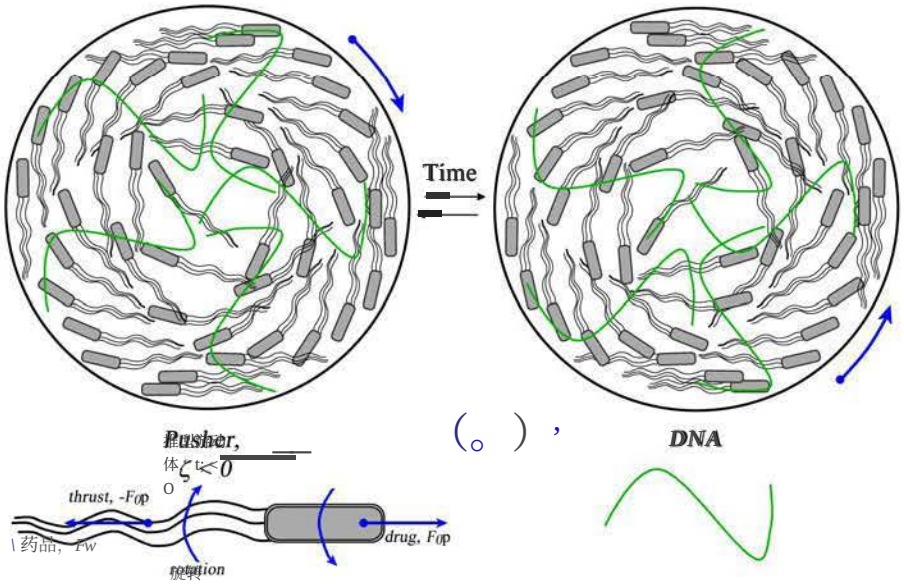

图1.9：少量DNA对游动细菌悬浮液流场产生显著影响的示意图。DNA大分子的存在会引发整个样品的旋转运动。在一段特定时间内，流动方向会从顺时针变为逆时针[96]。

Figure 1.9: Schematic representation of the dramatic effect of adding a small amount of DNA on the flow field of swimming bacterial suspensions. The presence of the DNA macromolecule induces the onset of a sample-spanning rotational motion. The direction of the flow field changes from clockwise to anti-clockwise over a defined time period[96].

The recent results obtained for active fluids in turbulent-like regime can be critically compared with previous investigations, focusing on polymer solutions. Grosiman and Steinberg[97,98] discovered that dilute solutions of high molecular weight polymers give rise to a sudden increase of the measured shear viscosity, as well as to turbulent-like features flow effects even at $Re << 1$ in either von Karman swirling disks or microfluidic curvilinear geometries, provided that the Weissenberg number $Wi = \lambda_1 \gamma$ is of order unity. Such Elastic Turbulence (E.T.) regime displays unique properties different from that of classical (inertial) turbulence.

Most remarkably, in E. T. the formation of a layer with enhanced magnitude of both local strain rate and velocity fluctuations (near the boundaries of the flow) was observed.[99] The width of such layer is Wi-independent, and varies only very weakly with the polymer concentration.[100] The maximum measured local strain rate within the boundary layer tends to saturate for sufficiently high values of Wi, which was related to a sudden coil-stretch transition of the polymer chains within the boundary layer, occurring at $Wi \approx 1$.[99] Therefore, the key features of the turbulent-like regime observed for active fluids (i.e., vanishing viscosity and appearance of

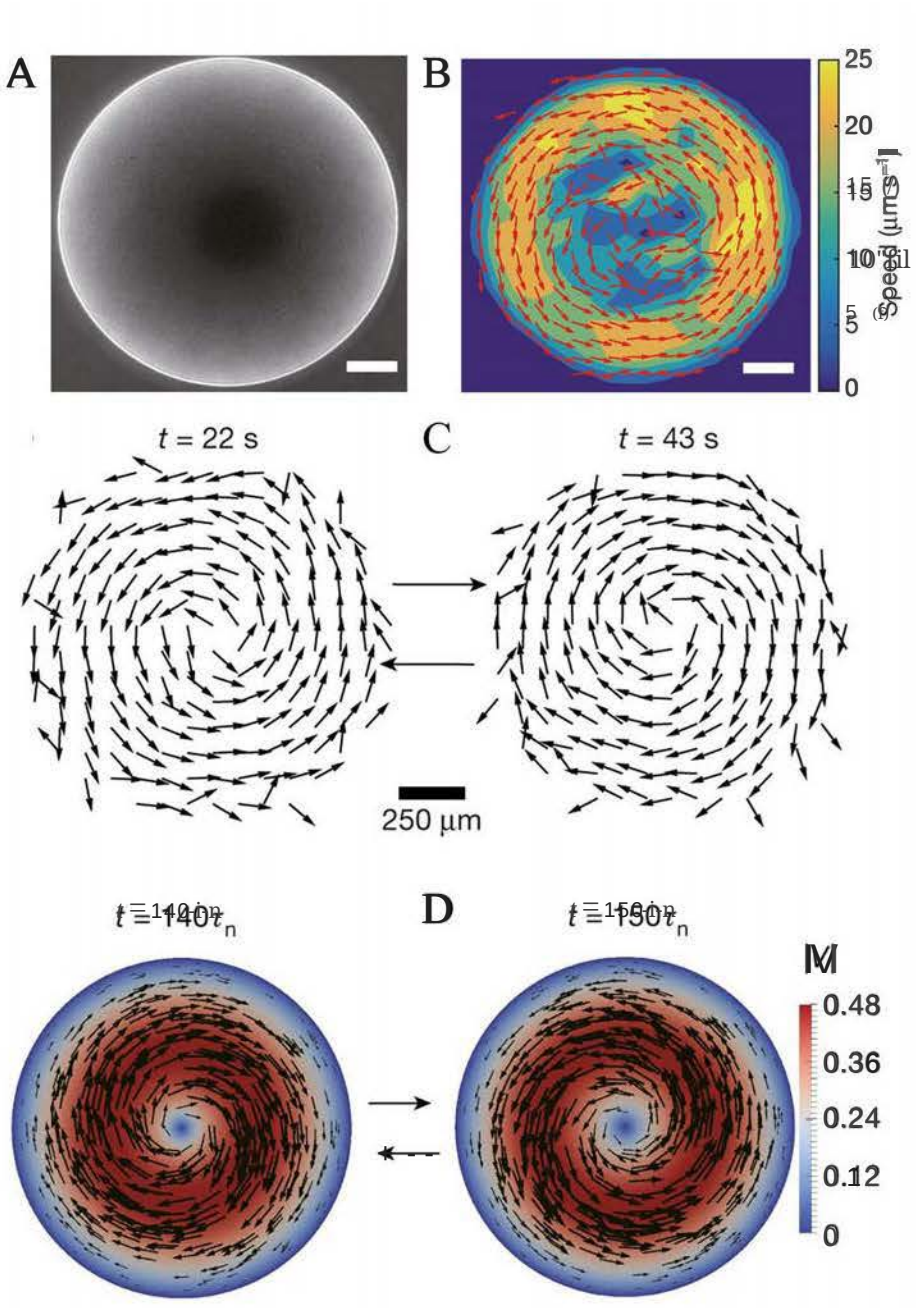

图1.10：在游动细菌悬浮液中加入少量DNA，对流场产生了显著影响。图1.10：(A)对比图像，以及
[illegible]
Figure 1.10: The dramatic effect of adding a small amount of DNA on the flow field of swimming
bacterial suspensions. Fig. 1.10: (A) contrast image and (B) instantaneous velocity field (B) the instantaneous
[illegible]
Fig. 1.10: (C) instantaneous velocity field and (D) velocity contour map of an oscillatory giant vortex
obtained by increasing DNA concentration up to 800 ng/mL. Adapted from Ref.[96] with permission from
[Springer Nature], Copyright [2021].

In light of these results, it is natural to ask under which conditions the addition of polymers, or swimmers of varying shape or type, can modify the observed turbulent-like flow structures. This question was addressed in the recent work of Liu *et al.*[96] where the effect of adding DNA to a dense suspension of *E. Coli* was investigated by means of a combination of particle-image velocimetry (PIV) and rheometry. When the DNA concentration exceeded 50 ng/μL, the observed flow structure transitioned from a disordered ensemble of small vortices to a single, system-spanning rotating vortex. With a further increase of the DNA concentration, the single vortex displays an oscillatory motion (see Fig. 1.9). These experimental data were also supported by simulations, which demonstrated that the observed transition from a rotating large vortex to an oscillating large vortex is driven by a balance between the active force exerted by the swimming bacteria and the viscoelasticity of the medium (see Fig. 1.10).

1.7 Perspectives

Over the past several decades, there has been an extraordinary progress in understanding the rheology of active fluids, arising mainly from theoretical research. Despite some promising experimental results, there is still a lack of rheological data concerning active particles in both Newtonian and non-Newtonian matrices. As discussed in Section 1.3, the viscosity measurements of pushers suspensions encounter key problems due to sensitivity limits of rotational rheometers. Microfluidic rheometers based on either flow visualisation [36,37] or on direct pressure sensing [101,102] have recently emerged as techniques that can successfully characterise the rheological properties of low viscosity fluids over a range of shear rates much larger than what can be explored by conventional techniques. It is envisaged that such techniques will be increasingly used to study the rheometric properties of active fluids.

It is worthy to highlight that examples of active fluids where the suspended particles are other than bacteria or artificial swimmers have not yet been properly addressed. For instance, protein-based active fluids have not yet received much attention from the scientific community. Motor proteins are mechanochemical enzymes that can move along the cytoplasm of animal cells. Their activity is due to the hydrolysis of adenosine triphosphate (ATP).[103] Kinesins, dyneins are motor proteins that can move actively along microtubules, while and myosins can move along actin filaments. Microtubule motors can be plus-end motors and minus-end motors, depending on the "walk" direction along the microtubule cables within the cell. Mofrad *et al.*[104] highlighted the unique aspect of the cytoskeleton for which active and passive characteristics need to be considered at the same time. Moreover, cytoskeletal structures are highly stimuli-responsive, which further complicates experimental measurements aiming at establishing material properties.[105]

The recent observations concerning the onset of non-linear flow for pusher suspensions in the super-fluid regime represents an exciting finding which has stimulated noteworthy research activity [39,70,96]. There is still a wide avenue for future work, specially focusing on the effect of polymer additives on the observed flow effects. The interaction between such collective bacterial motion and the well-known "Elastic Turbulence" regime observed if a small amount of polymer is added to the buffer[99,100] deserves a detailed investigation. Moreover, the

聚合物溶液的流变性质会随浓度跨越四种浓度区间（稀溶液、半稀未缠结、半稀缠结和浓缩）而显著变化，这种变化对细菌运动的影响应成为系统研究的重点。

rheological properties of polymer solutions vary significantly if the concentration is changed across four concentration regimes (dilute, semi-dilute unentangled, semi-dilute entangled and concentrated[106]), and the effect of such variation on the bacterial motion should constitute the focus of a systematic study.

References
参考文献

[1] M. Reiner, The Deborah Number, *Physics Today*, **1964**, **17**, 62。[2] G. S. Blair, 流变性质的分类, *Classification of rheological properties*, 1942。[3] C. Foias, O. Manley, R. Rosa 和 R. Temam, 《纳维-斯托克斯方程与湍流》, 剑桥大学出版社, 2001年, 第83卷。[4] V. M. Canuto, A. Howard, Y. Cheng 和 M. S. Dubovikov, 《海洋湍流》。第一部分：单点闭合模型~动量与热量的垂向扩散率, 《物理海洋学杂志》, 2001年6月1日, 31, 1413 - 1426。[5] A. Einstein, 博士论文, 苏黎世联邦理工学院, 1905年。[6] G. 巴彻勒, 具有流体动力学相互作用的粒子布朗扩散, 《流体力学杂志》, 1976年, 74, 1-29。[7] I. M. Krieger 和 T. J. Dougherty, 刚性球悬浮液中非牛顿流动的一种机制, 《流变学会会刊》, 1959年, 3, 137-152。[8] L. Gentile、B. F. Silva、S. Balog、K. Mortensen 和 U. Olsson, 剪切流与温度变化引起的非离子表面活性剂/水体系结构转变, 《胶体与界面科学杂志》, 2012年, 372, 32。[9] L. Gentile, B. F. Silva, S. Lages, K. Mortensen, J. Kohlbrecher 和 U. Olsson, 非离子层状相由的流变混沌与流动不稳定现象, 《Soft Matter》, 2013年, 9, 1133。[10] L. Giomi, T. B. Liverpool 和 M. C. Marchetti, 剪切活性流体：增稠、变稀与黏度消失, Physical Review E, 2010年, 81, 051908。[11] R. B. Bird、W. E. Stewart、E. N. Lightfoot 和 R. E. Meredith, 《输运现象》, 《电化学学会杂志》, 1961年, 108, 78C。[12] E. M. Purcell, 低雷诺数下的生命, 《美国物理学杂志》, 1977年, 45, 3-11。[13] J. E. Becker, S. A. Koehler 和 H. A. Stone, 低雷诺数下微型机器的自推进：Purcell 的三连杆游动体, 《流体力学杂志》, 2003年, 490, 15。[14] E. Lauga 和 T. R. Powers, 游动微生物的流体动力学, 《物理学进展报告》, 2009年, 72, 096601。[15] J. J. Higdon, 鞭毛推进的流体动力学分析, 《流体力学杂志》, 1979年, 90, 685-711。[16] S. F. Goldstein、N. W. Charon 和 J. A. Kreiling, 伯氏疏螺旋体以平面波形游动, 与真核生物鞭毛的波形相似, 《美国国家科学院院刊》, 1994年, 91, 3433-3437。[17] 《巴特沃思-海涅曼化学工程丛书》, S. Kim 和 S. J. Karrila 编, 巴特沃思-海涅曼出版社, 1991年, 第ii页。[18] S. Ghose 和 Adhikari, 活性软物质中振荡流与旋涡流的不可约表示, Physical Review Letters, 2014年, 112, 118102。

[1] M. Reiner, The Deborah Number, *Physics Today*, **1964**, **17**, 62.

[2] G. S. Blair, *Classification of rheological properties*, 1942.

[3] C. Foias, O. Manley, R. Rosa and R. Temam, *Navier-Stokes equations and turbulence*, Cambridge University Press, 2001, vol. 83.

[4] V. M. Canuto, A. Howard, Y. Cheng and M. S. Dubovikov, Ocean Turbulence. Part I: One-Point Closure Model—Momentum and Heat Vertical Diffusivities, *Journal of Physical Oceanography*, 01 Jun. 2001, **31**, 1413 – 1426.

[5] A. Einstein, *Inaug. Diss.*, Univ. Zurich, 1905.

[6] G. Batchelor, Brownian diffusion of particles with hydrodynamic interaction, *Journal of Fluid Mechanics*, 1976, **74**, 1–29.

[7] I. M. Krieger and T. J. Dougherty, A mechanism for non-Newtonian flow in suspensions of rigid spheres, *Transactions of the Society of Rheology*, 1959, **3**, 137–152.

[8] L. Gentile, B. F. Silva, S. Balog, K. Mortensen and U. Olsson, Structural transitions induced by shear flow and temperature variation in a nonionic surfactant/water system, *Journal of Colloid and Interface Science*, 2012, **372**, 32.

[9] L. Gentile, B. F. Silva, S. Lages, K. Mortensen, J. Kohlbrecher and U. Olsson, Rheochaos and flow instability phenomena in a nonionic lamellar phase, *Soft Matter*, 2013, **9**, 1133.

[10] L. Giomi, T. B. Liverpool and M. C. Marchetti, Sheared active fluids: Thickening, thinning, and vanishing viscosity, *Physical Review E*, 2010, **81**, 051908.

[11] R. B. Bird, W. E. Stewart, E. N. Lightfoot and R. E. Meredith, Transport phenomena, *Journal of the Electrochemical Society*, 1961, **108**, 78C.

[12] E. M. Purcell, Life at low Reynolds number, *American Journal of Physics*, 1977, **45**, 3–11.

[13] J. E. Becker, S. A. Koehler and H. A. Stone, On self-propulsion of micro-machines at low Reynolds number: Purcell's three-link swimmer, *Journal of Fluid Mechanics*, 2003, **490**, 15.

[14] E. Lauga and T. R. Powers, The hydrodynamics of swimming microorganisms, *Reports on Progress in Physics*, 2009, **72**, 096601.

[15] J. J. Higdon, A hydrodynamic analysis of flagellar propulsion, *Journal of Fluid Mechanics*, 1979, **90**, 685–711.

[16] S. F. Goldstein, N. W. Charon and J. A. Kreiling, Borrelia burgdorferi swims with a planar waveform similar to that of eukaryotic flagella., *Proceedings of the National Academy of Sciences*, 1994, **91**, 3433–3437.

[17] *Butterworth-Heinemann Series in Chemical Engineering*, ed. S. Kim and S. J. Karrila, Butterworth-Heinemann, 1991, p. ii.

[18] S. Ghose and R. Adhikari, Irreducible representations of oscillatory and swirling flows in active soft matter, *Physical Review Letters*, 2014, **112**, 118102.

[19] D. Saintillan, Rheology of Active Fluids, *Annual Review, Fluid Mechanics*, 2018, **50**, 563–588. [20] K. Drescher, J. Dunkel, L. H. Cisneros, S. Ganguly and R. E. Goldstein, Fluid dynamics and noise in bacterial cell–cell and cell–surface scattering, *Proceedings of the National Academy of Sciences*, 2011, **108**, 10940–10945. [21] E. Lauga, W. R. DiLuzio, G. M. Whitesides and H. A. Stone, Swimming in circles: motion of bacteria near solid boundaries, *Biophysical Journal*, 2006, **90**, 400–412. [22] J. Dunkel, S. Heidenreich, K. Drescher, H. H. Wensink, M. Bär and R. E. Goldstein, Fluid Dynamics of Bacterial Turbulence, *Physical Review Letters*, 2013, **110**, 228102. [23] J. Dunkel, S. Heidenreich, M. Bär and R. E. Goldstein, Minimal continuum theories of structure formation in dense active fluids, *New Journal of Physics*, 2013, **15**, 045016. [24] H. H. Wensink, J. Dunkel, S. Heidenreich, K. Drescher, R. E. Goldstein, H. Löwen and J. M. Yeomans, Meso-scale turbulence in living fluids, *Proceedings of the National Academy of Sciences*, 2012, **109**, 14308–14313. [25] J. Toner and Y. Tu, Flocks, herds, and schools: A quantitative theory of flocking, *Physical Review E*, 1998, **58**, 4828–4858. [26] J. Toner, Y. Tu and S. Ramaswamy, Hydrodynamics and phases of flocks, *Annals of Physics*, 2005, **318**, 170 – 244. [27] S. Ramaswamy, The Mechanics and Statistics of Active Matter, *Annual Review of Condensed Matter Physics*, 2010, **1**, 323–345. [28] L. H. Cisneros, J. O. Kessler, S. Ganguly and R. E. Goldstein, Dynamics of swimming bacteria: Transition to directional order at high concentration, *Physical Review E*, 2011, **83**, 061907. [29] L. H. Cisneros, R. Cortez, C. Dombrowski, R. E. Goldstein and J. O. Kessler, Fluid dynamics of self-propelled microorganisms, from individuals to concentrated populations, *Experiments on Fluids*, 2007, **43**, 737–753. [30] C. Dombrowski, L. Cisneros, S. Chatkaew, R. E. Goldstein and J. O. Kessler, Self-Concentration and Large-Scale Coherence in Bacterial Dynamics, *Physical Review Letters*, 2004, **93**, 098103. [31] R. Aditi Simha and S. Ramaswamy, Hydrodynamic fluctuations and instabilities in Ordered Suspensions of Self-Propelled Particles, *Physical Review Letters*, 2002, **89**, 058101. [32] K. Drescher, J. Dunkel, L. H. Cisneros, S. Ganguly and R. E. Goldstein, Fluid dynamics and noise in bacterial cell–cell and cell–surface scattering, *Proceedings of the National Academy of Sciences*, 2011, **108**, 10940–10945. [33] S. Heidenreich, P. Hilger and S. Hess, Boundary conditions for fluids with internal orientation, *Physical Review E*, 2007, **75**, 066302. [34] H. M. López, J. Gachelin, C. Douarche, H. Auradou and E. Clément, Turning Bacteria Suspensions into Superfluids, *Physical Review Letters*, 2015, **115**, 028301. [35] S. Rafaï, L. Jibuti and P. Peyla, Effective Viscosity of Microswimmer Suspensions, *Physical Review Letters*, 2010, **104**, 098102. [36] J. Gachelin, G. Miño, H. Berthet, A. Lindner, A. Rousselet and E. Clément, Non-Newtonian Viscosity of Escherichia coli Suspensions, *Physical Review Letters*, 2013, **110**, 268103.

[37] P. Guillot, P. Panizza, J.-B. Salmon, M. Joanicot, A. Colin, C.-H. Bruneau and T. Colin, 微流控装置中的黏度可调流体, *Langmuir*, 2006年, **22**, 6438-6445。[38] TA Instruments, *ARES 用户手册*, [39] V. A. Martinez, E. Clement, J. Arlt, C. Douarche, A. Dawson, J. Schwarz-Linek, A. K. Creppy, V. Skultéty, A. N. Morozov, H. Auradou and W. C. K. Poon, 细菌悬液黏度降低的流变测量与成像联合研究, *Proceedings of the National Academy of Sciences*, 2020年, 117, 2326-2331。[40] P. S. Sarangapani, J. Weaver, A. Parupudi, T. M. Besong, G. G. Adams, S. E. Harding, P. Manikwar, M. M. Castellanos, S. M. Bishop and J. A. Pathak, 可逆自缔合和结构变化共同构成单克隆抗体溶液分子黏弹性的基础, *《药学科学杂志》*, 2016年, 105, 3496-3506。[41] Y. Hatwalne, S. Ramaswamy, M. Rao and R. A. Simha, 活性粒子悬浮液的流变学, Phys. Rev. Lett., 2004年, 92, 118101。[42] A. Sokolov and I. S. Aranson, 游动细菌悬浮液的黏度降低, *《物理评论快报》*, 2009年, 103, 148101。[43] D. Saintillan, 游动悬浮液的稀悬浮流变学: 简单运动学模型, *Experimental Mechanics*, 2010年, 50, 1275-1281。[44] D. Saintillan and M. J. Shelley, 自推进杆状粒子悬浮液中的取向有序与不稳定性, Phys. Rev. Lett., 2007年, 99, 058102。[45] V. MEHANDIA and P. R. NOTT, 自驱动粒子的集体动力学, *《流体力学杂志》*, 2008年, 595, 239-264。[46] J. P. Hernandez-Ortiz, C. G. Stoltz and M. D. Graham, 受限游动粒子悬浮液中的输运与集体动力学, *《物理评论快报》*, 2005年, 95, 204501。[47] A. Patteson, A. Gopinath, M. Goulian and P. Arratia, 聚合物溶液中大肠杆菌的奔跑与翻滚, *《科学报告》*, 2015年, 5, 15761。[48] J. Saragosti, P. Silberzan and A. Buguin, 通过转动扩散模拟大肠杆菌的翻滚：对趋化性的影响, *《公共科学图书馆·综合》*, 2012年, 7, 1-6。[49] M. MuBler, 莱茵衣藻微型游动体的流变学与流体动力学: 活性流体模型, 2014年。[50] L. Giomi, T. B . Liverpool and M. C. Marchetti, 剪切活性流体：增稠、变稀与黏度消失, Physical Review E, 2010年, 81, 051908。[51] G. Foffano, J. S. Lintuvuori, A. N. Morozov, K. Stratford, M. E. Cates and D. Marenduzzo, 活性流体的体相流变学与微流变学, *《欧洲物理学杂志E》*, 2012年, 35, .。[52] R. Karmakar, R. Gulvady, M. S. Tirumkudulu and K. V. Venkatesh, 马达特性决定微型游动体悬浮液的流变行为, *《流体物理学》*, 2014年, 26, 071905。[53] J. Möller, T. Luehmann, H. Hall and V. Vogel, 《极点竞速：高长径比形状和异质环境如何限制巨噬细胞对丝状大肠杆菌的吞噬作用》, *《纳米快报》*, 2012年, 12, 2901-2905。[54] M. Mussler, S. Rafai, P. Peyla and C. Wagner, 非重力趋性莱茵衣藻微型游泳者悬浮液的有效黏度, EPL（Europhysics Letters）, 2013年, 101, 54004。

[37] P. Guillot, P. Panizza, J.-B. Salmon, M. Joanicot, A. Colin, C.-H. Bruneau and T. Colin, Viscosity bifurcation of a suspension of drops flowing in a microfluidic T-junction, *Langmuir*, 2006, **22**, 6438–6445.

[38] TA Instruments, *ARES Rheometer Manual*.

[39] V. A. Martinez, E. Clement, J. Arlt, C. Douarche, A. Dawson, J. Schwarz-Linek, A. K. Creppy, V. Skultéty, A. N. Morozov, H. Auradou and W. C. K. Poon, A combined rheometry and imaging study of viscosity reduction in bacterial suspensions, *Proceedings of the National Academy of Sciences*, 2020, **117**, 2326–2331.

[40] P. S. Sarangapani, J. Weaver, A. Parupudi, T. M. Besong, G. G. Adams, S. E. Harding, P. Manikwar, M. M. Castellanos, S. M. Bishop and J. A. Pathak, Both reversible self-association and structural changes underpin molecular viscoelasticity of mAb solutions, *Journal of Pharmaceutical Sciences*, 2016, **105**, 3496–3506.

[41] Y. Hatwalne, S. Ramaswamy, M. Rao and R. A. Simha, Rheology of Active-Particle Suspensions, *Phys. Rev. Lett.*, 2004, **92**, 118101.

[42] A. Sokolov and I. S. Aranson, Reduction of Viscosity in Suspension of Swimming Bacteria, *Physical Review Letters*, 2009, **103**, 148101.

[43] D. Saintillan, The Dilute Rheology of Swimming Suspensions: A Simple Kinetic Model, *Experimental Mechanics*, 2010, **50**, 1275–1281.

[44] D. Saintillan and M. J. Shelley, Orientational Order and Instabilities in Suspensions of Self-Locomoting Rods, *Phys. Rev. Lett.*, 2007, **99**, 058102.

[45] V. MEHANDIA and P. R. NOTT, The collective dynamics of self-propelled particles, *Journal of Fluid Mechanics*, 2008, **595**, 239–264.

[46] J. P. Hernandez-Ortiz, C. G. Stoltz and M. D. Graham, Transport and Collective Dynamics in Suspensions of Confined Swimming Particles, *Physical Review Letters*, 2005, **95**, 204501.

[47] A. Patteson, A. Gopinath, M. Goulian and P. Arratia, Running and tumbling with *E. coli* in polymeric solutions, *Sci. Rep.*, 2015, **5**, 15761.

[48] J. Saragosti, P. Silberzan and A. Buguin, Modeling *E. coli* Tumbles by Rotational Diffusion. Implications for Chemotaxis, *PLOS ONE*, 2012, **7**, 1–6.

[49] M. MuBler, *Rheologie und Hydrodynamik des Mikroschwimmers Chlamydomonas reinhardtii als Modell für aktive Fluide*, 2014.

[50] L. Giomi, T. B. Liverpool and M. C. Marchetti, Sheared active fluids: Thickening, thinning, and vanishing viscosity, *Physical Review E*, 2010, **81**, 051908.

[51] G. Foffano, J. S. Lintuvuori, A. N. Morozov, K. Stratford, M. E. Cates and D. Marenduzzo, Bulk rheology and microrheology of active fluids, *The European Physical Journal E*, 2012, **35**, .

[52] R. Karmakar, R. Gulvady, M. S. Tirumkudulu and K. V. Venkatesh, Motor characteristics determine the rheological behavior of a suspension of microswimmers, *Physics of Fluids*, 2014, **26**, 071905.

[53] J. Möller, T. Luehmann, H. Hall and V. Vogel, The Race to the Pole: How High-Aspect Ratio Shape and Heterogeneous Environments Limit Phagocytosis of Filamentous Escherichia coli Bacteria by Macrophages, *Nano Letters*, 2012, **12**, 2901–2905.

[54] M. Mussler, S. Rafaï, P. Peyla and C. Wagner, Effective viscosity of non-gravitactic Chlamydomonas Reinhardtii microswimmer suspensions, *EPL (Europhysics Letters)*, 2013, **101**, 54004.

[55] D. Saintillan and M. J. Shelley, Emergence of coherent structures and large-scale flows in motile suspensions, *Journal of The Royal Society Interface*, 2012, **9**, 571–585. [56] V. O. Adesanya, D. C. Vadillo and M. R. Mackley, The rheological characterization of algae suspensions for the production of biofuels, *Journal of Rheology*, 2012, **56**, 925–939.
[57] R. Jeanneret, D. O. Pushkin and M. Polin, Confinement Enhances the Diversity of Microbial Flow Fields, *Physical Review Letters*, 2019, **123**, 248102.
[58] S. Antoine, P. Jeremy, L. Jack, C. Cathy and B. Teodor, Rheological properties of suspensions of the alga Haematococcus pluvialis at various volume fractions, *Rheologica Acta*, 2013, **52**, 589–605.
[59] S. Mueller, E. W. Llewellin and H. M. Mader, The rheology of suspensions of solid particles, *Proceedings of the Royal Society A: Mathematical, Physical and Engineering Sciences*, 2010, **466**, 1201–1228.
[60] N. Cagney, I. Zhang, R. Bransgrove, M. Allen and S. Balabani, Effects of cell motility and morphology on the rheology of algae suspensions, *Journal of Applied Phycology*, 2017, **29**, 2241–2257.
[61] A. Wileman, A. Ozkan and H. Berberoglu, Rheological properties of algae slurries for minimizing harvesting energy requirements in biofuel production, *Bioresource Technology*, 2012, **104**, 432–439.
[62] Z. Wu and X. Shi, Rheological properties of Chlorella pyrenoidosa culture grown heterotrophically in a fermentor, *Journal of Applied Phycology*, 2008, **20**, 279–282.
[63] X. Zhang, Z. Jiang, L. Chen, A. Chou, H. Yan, Y. Y. Zuo and X. Zhang, Influence of cell properties on rheological characterization of microalgae suspensions, *Bioresource Technology*, 2013, **139**, 209–213.
[64] Z. Liu, K. Zhang and X. Cheng, Rheology of bacterial suspensions under confinement, *Rheologica Acta*, 2019, **58**, 439–451.
[65] B. M. Haines, A. Sokolov, I. S. Aranson, L. Berlyand and D. A. Karpeev, Three-dimensional model for the effective viscosity of bacterial suspensions, *Physical Review E*, 2009, **80**, 041922.
[66] D. Saintillan, The dilute rheology of swimming suspensions: A simple kinetic model, *Experimental Mechanics*, 2010, **50**, 1275–1281.
[67] S. D. Ryan, B. M. Haines, L. Berlyand, F. Ziebert and I. S. Aranson, Viscosity of bacterial suspensions: Hydrodynamic interactions and self-induced noise, *Physical Review E*, 2011, **83**, 050904.
[68] M. Moradi and A. Najafi, Rheological properties of a dilute suspension of self-propelled particles, *EPL (Europhysics Letters)*, 2015, **109**, 24001.
[69] L. Gentile and S. Amin, in *Colloidal Foundations of Nanoscience 2nd Edition*, ed. D. Berti and G. Palazzo, Elsevier, 2021, ch. 11.
[70] S. Guo, D. Samanta, Y. Peng, X. Xu and X. Cheng, Symmetric shear banding and swarming vortices in bacterial superfluids, *Proceedings of the National Academy of Sciences*, 2018, **115**, 7212–7217.
[71] C. R. Doering and J. D. Gibbon, *Applied Analysis of the Navier-Stokes Equations*, Cambridge University Press, 1995.
[72] M. Cates, S. Fielding, D. Marenduzzo, E. Orlandini and J. Yeomans, Shearing active gels close to the isotropic-nematic transition, *Physical Review Letters*, 2008, **101**, 068102.

[73] C. Hohenegger and M. J. Shelley, Stability of active suspensions, *Physical Review E*, 2010年, *E*, 81, 046311。[74] M. Theillard、R. Alonso-Matilla 和 D. Saintillan，活性集体运动的几何控制，Soft Matter，2017年，13，363-375。[75] G. Negro、L. N. Carenza、A. Lamura、A. Tiribocchi 和 G. Gonnella，活性极性乳液的流变学：从线性流动到单向流动和无黏流动，以及间歇性黏度，Soft Matter，2019年，15，8251-8265。[76] F. Bonelli、L. N. Carenza、G. Gonnella、D. Marenduzzo、E. Orlandini 和 A. Tiribocchi，奇异活性乳液中的层状有序化、液滴形成和相反转，Scientific Reports，2019年，9，1-11。[77] L. N. Carenza、L. Biferale 和 G. Gonnella，活性乳液动力学的多尺度控制，Physical Review Fluids，2020年，5，year。[78] J. P. Celli、B. S. Turner、N. H. Afdhal、S. Keates、I. Ghiran、C. P. Kelly、R. H. Ewoldt、G. H. McKinley、P. So、S. Erramilli 和 R. Bansil，幽门螺杆菌通过降低黏度在白黏蛋性黏液中移动，Proceedings of the National Academy of Sciences，2009年，106，14321-14326。[79] L. J. Fauci 和 R. Dillon，《生殖生物流体力学》，Annual Review of Fluid Mechanics，2006年，38，371-394。[80] M. Brust、C. Schaefer、R. Doerr、L. Pan、M. Garcia、P. E. Arratia 和 C. Wagner，人血浆的流变学：黏弹性行为与牛顿行为，Physical Review Letters，2013年，110，078305。[81] C. Viscoli，血流感染：冰山一角，Virulence，2016年，7，248-251。[82] M. Rubinstein、R. H. Colby 等，《聚合物物理学》，牛津大学出版社，纽约，2003年，第23卷。[83] L. E. Rodd、T. P. Scott、D. V. Boger、J. J. Cooper-White 和 G. H. McKinley，微加工几何结构中低黏度弹性流体的惯性-弹性平面入口流，Journal of Non-Newtonian Fluid Mechanics，2005年，129，1-22。[84] A. Lanzaro 和 X. F. Yuan，微流控中平稳伸、高度多分散聚丙烯酰胺溶液的收缩比对非线性动力学的影响，Journal of Non-Newtonian Fluid Mechanics，2011年，166，1064-1075。[85] R. G. Larson，柔性聚合物稀溶液的流变学：进展与问题，Journal of Rheology，2005年，49，1-70。[86] E. Lauga，高德博拉数下的生命，EPL（Europhysics Letters），2009年，86，64001。[87] R. G. Owens 和 T. N. Phillips，计算流变学，World Scientific，2002年。[88] N. C. Keim，流体弹性能够在低雷诺数下实现推进，《流体物理学》，2012年，24，081703。[89] T. Qiu、S. Palagi、A. G. Mark、K. Melde、F. Adams 和 P. Fischer，利用功能声学表面实现无线驱动，Applied Physics Letters，2016年，109，191602。[90] P. Pakdel 和 G. H. McKinley，弹性失稳与弯曲流线，《物理评论快报》，1996年，77，2459-2462。[91] G. H. McKinley、P. Pakdel 和 A. Öztekin，纯弹性流动失稳的流变学与几何标度，Journal of Non-Newtonian Fluid Mechanics，1996年，67，19-47。[92] D. A. Gagnon、N. C. Keim、X. Shen 和 P. E. Arratia，蠕虫状胶束溶液中流体诱导的刚性颗粒推进，《流体物理学》，2014年，26，103101。

[73] C. Hohenegger and M. J. Shelley, Stability of active suspensions, *Physical Review E*, 2010, **81**, 046311.

[74] M. Theillard, R. Alonso-Matilla and D. Saintillan, Geometric control of active collective motion, *Soft Matter*, 2017, **13**, 363–375.

[75] G. Negro, L. N. Carenza, A. Lamura, A. Tiribocchi and G. Gonnella, Rheology of active polar emulsions: from linear to unidirectional and inviscid flow, and intermittent viscosity, *Soft Matter*, 2019, **15**, 8251–8265.

[76] F. Bonelli, L. N. Carenza, G. Gonnella, D. Marenduzzo, E. Orlandini and A. Tiribocchi, Lamellar ordering, droplet formation and phase inversion in exotic active emulsions, *Scientific Reports*, 2019, **9**, 1–11.

[77] L. N. Carenza, L. Biferale and G. Gonnella, Multiscale control of active emulsion dynamics, *Physical Review Fluids*, 2020, **5**, year.

[78] J. P. Celli, B. S. Turner, N. H. Afdhal, S. Keates, I. Ghiran, C. P. Kelly, R. H. Ewoldt, G. H. McKinley, P. So, S. Erramilli and R. Bansil, Helicobacter pylori moves through mucus by reducing mucin viscoelasticity, *Proceedings of the National Academy of Sciences*, 2009, **106**, 14321 – 14326.

[79] L. J. Fauci and R. Dillon, BIOFLUIDMECHANICS OF REPRODUCTION, *Annual Review of Fluid Mechanics*, 2006, **38**, 371–394.

[80] M. Brust, C. Schaefer, R. Doerr, L. Pan, M. Garcia, P. E. Arratia and C. Wagner, Rheology of Human Blood Plasma: Viscoelastic Versus Newtonian Behavior, *Physical Review Letters*, 2013, **110**, 078305.

[81] C. Viscoli, Bloodstream infections: The peak of the iceberg, *Virulence*, 2016, **7**, 248–251.

[82] M. Rubinstein, R. H. Colby *et al.*, *Polymer Physics*, Oxford university press New York, 2003, vol. 23.

[83] L. E. Rodd, T. P. Scott, D. V. Boger, J. J. Cooper-White and G. H. McKinley, The inertio-elastic planar entry flow of low-viscosity elastic fluids in micro-fabricated geometries, *Journal of Non-Newtonian Fluid Mechanics*, 2005, **129**, 1 – 22.

[84] A. Lanzaro and X. F. Yuan, Effects of contraction ratio on non-linear dynamics of semi-dilute, highly polydisperse polyacrylamide solutions in microfluidics, *Journal of Non-Newtonian Fluid Mechanics*, 2011, **166**, 1064–1075.

[85] R. G. Larson, The rheology of dilute solutions of flexible polymers: Progress and problems, *Journal of Rheology*, 2005, **49**, 1–70.

[86] E. Lauga, Life at high Deborah number, *EPL (Europhysics Letters)*, 2009, **86**, 64001.

[87] R. G. Owens and T. N. Phillips, *Computational rheology*, World Scientific, 2002.

[88] N. C. Keim, Fluid elasticity can enable propulsion at low Reynolds number, *Physics of Fluids*, 2012, **24**, 081703.

[89] T. Qiu, S. Palagi, A. G. Mark, K. Melde, F. Adams and P. Fischer, Wireless actuation with functional acoustic surfaces, *Applied Physics Letters*, 2016, **109**, 191602.

[90] P. Pakdel and G. H. McKinley, Elastic Instability and Curved Streamlines, *Physical Review Letters*, 1996, **77**, 2459–2462.

[91] G. H. McKinley, P. Pakdel and A. Öztekin, Rheological and geometric scaling of purely elastic flow instabilities, *Journal of Non-Newtonian Fluid Mechanics*, 1996, **67**, 19 – 47.

[92] D. A. Gagnon, N. C. Keim, X. Shen and P. E. Arratia, Fluid-induced propulsion of rigid particles in wormlike micellar solutions, *Physics of Fluids*, 2014, **26**, 103101.

[93] R. Kan、C. W. Shields、B. Bharti、P. Lara、A. Ortiz 和 O. D. Velev，非牛顿流体中磁组装“微型扇贝”的主动可逆游动，Langmuir，2020年，36，7148-7154。[94] J. R. Gomez-Solano、A. Blokhuis 和 C. Bechinger，黏弹性流体中自推进 Janus 粒子的动力学，《物理评论快报》，2016年，116，138301。[95] J. Hu、S. Zhou、Y. Sun、X. Fang 和 L. Wu，Janus 粒子的制备、性质与应用，《化学学会评论》，2012年，41，4356-4378。[96] S. Liu、S. Shankar、M. C. Marchetti 和 Y. Wu，黏弹性对细菌活性物质时空有序性的控制，《自然》，2021年，590，80-84。[97] A. Groisman 和 V. Steinberg，聚合物溶液流中的弹性湍流，《自然》，2000年，405，53-55。[98] A. Groisman 和 V. Steinberg，利用聚合物添加剂在低雷诺数下实现高效混合，《自然》，2001年，410，905-908。[99] T. Burghelea、E. Segre 和 V. Steinberg，两个圆盘之间冯·卡门旋转流中的弹性湍流，《流体物理学》，2007年，19，053104。[100] Y. Jun 和 V. Steinberg，冯·卡门旋转流中聚合物浓度与弹性湍流的性质，Physical Review Fluids，2017年，2，103301。[101] C. J. Pipe 和 G. H. McKinley，微流控流变测量，Mechanics Research Communications，2009年，36，110-120。[102] A. Lanzaro、D. Corbett 和 X.-F. Yuan，微流控三维十字槽流动几何中半稀释聚丙烯酰胺溶液的非线性动力学，Journal of Non-Newtonian Fluid Mechanics，2017年，242，57---65。[103] M. A. Hoyt、A. A. Hyman 和 M. Bahler，真核细胞骨架的马达蛋白，Proceedings of the National Academy of Sciences，1997年，94，12747-12748。[104] M. R. Mofrad，细胞骨架流变学，Annual Review of Fluid Mechanics，2009年，41，433-453。[105] D. Wirtz，活细胞的粒子追踪微流变学：原理与应用，Annual Review of Biophysics，2009年，38，301-326。[106] Y. Liu、Y. Jun 和 V. Steinberg，稀释和半稀释聚合物溶液最长弛豫时间的浓度依赖性，Journal of Rheology，2009年，53，1069-1085。

[93] R. Kan, C. W. Shields, B. Bharti, P. Lara, A. Ortiz 和 O. D. Velev, 非牛顿流体中磁组装“微型扇贝”的主动可逆游动，Langmuir，2020年，36，7148-7154。[94] J. R. Gomez-Solano、A. Blokhuis 和 C. Bechinger，黏弹性流体中自推进 Janus 粒子的动力学，《物理评论快报》，2016年，116，138301。[95] J. Hu、S. Zhou、Y. Sun、X. Fang 和 L. Wu，Janus 粒子的制备、性质与应用，《化学学会评论》，2012年，41，4356-4378。[96] S. Liu、S. Shankar、M. C. Marchetti 和 Y. Wu，黏弹性对细菌活性物质时空有序性的控制，《自然》，2021年，590，80-84。[97] A. Groisman 和 V. Steinberg，聚合物溶液流中的弹性湍流，《自然》，2000年，405，53-55。[98] A. Groisman 和 V. Steinberg，利用聚合物添加剂在低雷诺数下实现高效混合，《自然》，2001年，410，905-908。[99] T. Burghelea、E. Segre 和 V. Steinberg，两个圆盘之间冯·卡门旋转流中的弹性湍流，《流体物理学》，2007年，19，053104。[100] Y. Jun 和 V. Steinberg，冯·卡门旋转流中聚合物浓度与弹性湍流的性质，Physical Review Fluids，2017年，2，103301。[101] C. J. Pipe 和 G. H. McKinley，微流控流变测量，Mechanics Research Communications，2009年，36，110-120。[102] A. Lanzaro、D. Corbett 和 X.-F. Yuan，微流控三维十字槽流动几何中半稀释聚丙烯酰胺溶液的非线性动力学，Journal of Non-Newtonian Fluid Mechanics，2017年，242，57---65。[103] M. A. Hoyt、A. A. Hyman 和 M. Bahler，真核细胞骨架的马达蛋白，Proceedings of the National Academy of Sciences，1997年，94，12747-12748。[104] M. R. Mofrad，细胞骨架流变学，Annual Review of Fluid Mechanics，2009年，41，433-453。[105] D. Wirtz，活细胞的粒子追踪微流变学：原理与应用，Annual Review of Biophysics，2009年，38，301-326。[106] Y. Liu、Y. Jun 和 V. Steinberg，稀释和半稀释聚合物溶液最长弛豫时间的浓度依赖性，Journal of Rheology，2009年，53，1069-1085。

[105] D. Wirtz, Particle-tracking microrheology of living cells: principles and applications, *Annual Review of Biophysics*, 2009, **38**, 301–326.

[106] Y. Liu, Y. Jun and V. Steinberg, Concentration dependence of the longest relaxation times of dilute and semi-dilute polymer solutions, *Journal of Rheology*, 2009, **53**, 1069–1085.